**Title**
MOLECULAR BEAM SCATTERING FROM SOLID SURFACES



**Authors**
Bernasek, S.L.
Somorjai, G.A.

**Publication Date**
1974-03-01

Chapter in "Progress in Surface Science," Sidney G. Davison, ed., Pergamon Press



LBL-2591
Preprint

# MOLECULAR BEAM SCATTERING FROM SOLID SURFACES

S. L. Bernasek and G. A. Somorjai

March 1974

Prepared for the U. S. Atomic Energy Commission
under Contract W-7405-ENG-48



## DISCLAIMER

# MOLECULAR BEAM SCATTERING FROM SOLID SURFACES

S. L. Bernasek and G. A. Somorjai

Department of Chemistry and Inorganic Materials Research Division,
Lawrence Berkeley Laboratory, University of California
Berkeley, California, U.S.A.

CONTENTS

## 1. Introduction

The fundamental problem in the study of the gas-solid interaction is the elucidation of the energy exchange between the solid and the gas. An understanding of the chemistry and physics of the solid-gas interaction is necessary to an understanding of such processes as heterogeneous catalysis, corrosion, vapor deposition, cloud formation, condensation, satellite dynamics in rarified gases, and space simulation. In the study of the chemistry and physics of surfaces, the energy exchange between the gas and solid phases is a fundamental problem of interest. More specifically, the problem is to determine the microscopic initial and final energy states of the gas-solid system. This problem is illustrated schematically in Figure 1. An incident particle in the gas phase, in the state $E_i$, collides with a solid in the state $E_i'$. After the collision, the particle is in state $E_f$, while the solid is in the energy state $E_f'$. Depending on the nature of the incident particle, $E_i$ can be a sum of translational, rotational, vibrational and electronic states. $E_i'$ depends on the structure and composition, the temperature, and various other parameters of the solid lattice. After the interaction, the incident particle can leave the solid surface in the same state, in a different (higher or lower energy) state, it can become a part of the solid surface, or it can leave the surface as a chemically different species. The solid surface can, after the interaction, be in the same state as it was initially, it can be in a different energy state, it can be changed chemically by the interaction, or surface atoms can leave the solid and enter the gas phase as a result of a gas-surface chemical reaction.

The problem of determining the molecular details of the gas-solid energy exchange is indeed a difficult one for three reasons:

(1) The difficulty of characterizing the initial and final states of the system, especially that of the solid surface.

(2) The necessity to use approximate, often unrealistic, theories due to the intractability of the many-body quantum mechanical calculations which apply.

(3) The experimental difficulties arising from dealing with surface interactions.

An especially fruitful experimental technique for studying this energy exchange has been molecular beam scattering from solid surfaces. This review will deal with the study of the gas-solid energy exchange by molecular beam scattering techniques with particular emphasis on experimental work in the last ten years, 1964 to the latter part of 1973. The very early work in this field has been reviewed by Ramsey,[1] and reviews by Hurlbut[2] and Stickney[3] cover studies carried out in the early 1960's. Recent reviews by Merrill[4] and J. N. Smith[5] emphasize particular aspects of the field. Theoretical aspects of the problem will be dealt with in less detail than the experimental work. References to excellent review articles and extensive references to the original work are included in Section 2. Section 2 contains a discussion of the major theoretical treatments pertinent to the energy exchange in the gas surface interaction. Comparison of theory with the experimental work is described in Section 4. Section 3 discusses experimental techniques of studying the energy exchange which fall into the broad category of beam scattering methods. Section 4 looks at the

experimental work in this field during the last ten years with the purpose of collecting and organizing the information that has been gained about energy exchange in the gas-solid interaction utilizing molecular beam scattering from solid surfaces. Section 5 summarizes the results of the preceding sections and indicates the direction molecular beam scattering investigations should proceed in order to shed more light on a very important problem of surface science, i.e., the energetics of gas-surface interactions. This field is producing exciting results and developing rapidly.

## 2. Theories of Energy Exchange

### A. Accommodation Coefficient Theory

A quantitative description of the total energy transfer between a solid surface and an incident gas can be given by a quantity called the accommodation coefficient. The accommodation coefficient $\alpha$ is defined as:

$$\alpha \equiv \frac{E - E_2}{E_1 - E_2} \tag{1}$$

where $E_2$ is the energy of the incident gas, E is the energy of the reflected gas, and $E_1$ is the energy the reflected gas would have if it were in equilibrium with the surface at temperature $T_1$. If all of the energy is translational (monatomic gas) then $E_i = 2kT_iN$, using the Boltzmann distribution with N the number of particles per unit area per unit time. This allows the accommodation coefficient to be written in terms of temperatures.

$$\alpha = \frac{T - T_2}{T_1 - T_2} \tag{2}$$

For molecules with internal degrees of freedom, a translational and internal energy accommodation coefficient can be defined.

$$\alpha_t = \frac{T_t - T_2}{T_1 - T_2} \qquad \alpha_i = \frac{T_i - T_2}{T_1 - T_2} \tag{3}$$

where $T_t$ and $T_i$ are the temperatures related through the appropriate distributions to the translational and internal energies of the scattered gas. As can easily be seen, $\alpha$ approaches unity for complete energy transfer.

Experimental determinations of the accommodation coefficient have been made for many years by non-molecular beam methods.[7-9] Of course, a molecular beam apparatus capable of measuring the initial and final energy states of the gas scattering from the surface is the ideal apparatus for measuring the accommodation coefficient. Because of this compatibility of the molecular beam technique to accommodation coefficient measurement and because the theories form a background for more detailed energy transfer theories, this section will review briefly some of the theories of the accommodation coefficient.

The work of Goodman[10-12] in the early 1960's centered on classical mechanical calculations of the accommodation coefficient based on an n-dimensional semi-infinite lattice model. The model results indicated a lower accommodation coefficient for the three-dimensional case and included the possibility of trapping of the atom at the surface. Quantitative agreement was obtained with several rare gas-metal experimental systems. An interesting result of the calculation of the velocity distribution function of the reflected gas based on this theory is that the accommodation coefficient is not restricted to lie between zero and unity.[12]

The above model, and most other theoretical treatments of the accommodation coefficient, are based on perfectly clean surfaces. Since most accommodation coefficient measurements have been made on surfaces likely to be contaminated by impurities, the effect of impurities on the theoretical calculations is indeed an important point. McCarroll,[13] in a one-dimensional semi-infinite lattice calculation, found that adsorption of light atoms on the clean surface increased the accommodation coefficient. This is found to be the case for impurity coverages as low as 1%.[14] Allen

and Feuer[15] discuss this effect in terms of localized modes due to the impurity, which greatly increase the energy transfer. Evidence for this interpretation has been obtained in this laboratory while studying the nature of energy exchange between diatomic gases and clean and contaminated surfaces.[16] It was found that a platinum surface contaminated by CO gave rise to cosine scattering distributions for a variety of gases, while clean surfaces gave peaked distributions. (See Fig. 2.) The difference can be ascribed to low frequency bending modes of the adsorbed CO, which can absorb the incident gas translational energy.

The possibility of energy transfer via internal channels of the incident molecule has not received as much theoretical attention as translational energy transfer. Feuer[17] has proposed a quantum mechanical theory for rigid rotors scattered from a solid. He finds that in most cases $\alpha_i$ is considerably less than $\alpha_t$. This calculation will be discussed in a later section dealing with experimental inelastic scattering results.

Other classical mechanical treatments of the accommodation coefficient are given by Chambers and Kinzer,[18,19] and Armand.[20] Logan[21] uses the soft cube model to calculate $\alpha$ for rare gas scattering from tungsten. This model is discussed in greater detail in a later section. Based on this model, the fraction of incident atoms trapped at the surface can be calculated. It is found that the accommodation coefficient increases for higher trapping fractions in agreement with the results discussed above.

More complex classical treatments [22-24] of the accommodation coefficient, as well as quantum mechanical calculations [25-28] related to the Lennard-Jones Devonshire theory discussed in the following section, have been advanced. The theory of accommodation coefficients has not progressed to the point of routine first principles calculations of $\alpha$ for a given gas solid system. Semi-empirical formulas for $\alpha$ have been proposed,[22] and the theory as it now stands provides a physical insight to the qualitative nature of accommodation coefficient determinations. The use of molecular beam techniques for the precise determination of $\alpha$ from well characterized surfaces should stimulate further theoretical developments.

## B. Early Quantum Theory

The first quantum mechanical treatments of the energy exchange in gas-surface scattering were stimulated by the experiments of Stern and his coworkers[29,30] in the early 1930's. These early theories due to Devonshire, Lennard-Jones and Strachan[31-33] have laid the foundation for the more complex and physically interesting theories of the last several years. This section will briefly discuss the derivation of the early theory in order to give the reader an introduction to the nomenclature and reasoning used in the later quantum theories which will also be discussed.

Figure 3 describes the quantum mechanical problem which is to be solved. $p_i$ is the incident particle momentum with perpendicular component $p_{iz}$ and tangential component $P_i$. $\theta_i$ is the angle of incidence, $\theta_f$ is the scattering angle, and $\Phi_f$ is the out of plane angle. $\Phi_i$, the incident tangential angle, is chosen to be zero. $p_f$ is the scattered particle momentum with components $p_{fz}$ and $P_f$, and Z is the phonon momentum with components $q_z$ and Q.

For direct inelastic scattering (energy transfer occurs between solid and gas) the initial and final states of the gas atom are eigenstates of the assumed gas-surface potential. The theory of Lennard-Jones, Devonshire and Strachan treats the interaction of a single gas atom with a single surface atom. The tangential momentum of the gas atom is assumed unchanged by the encounter and the surface atom is assumed to behave as though it were in the bulk of an infinite three-dimensional Debye solid. A Morse potential is assumed for the interaction between the gas and surface atoms. The theory is developed by a first order

perturbation treatment, so the inelastically scattered intensity must be small compared to the incident particle intensity.

The system is a one-dimensional box of length L oriented along the z axis. $z = 0$ is the equilibrium position of the surface atom, $z > 0$ is the gas atom region, and $z < 0$ is the solid. The Morse potential is $V(z) = \Delta(e^{-2az} - 2e^{-az})$ where $\Delta$ and a are parameters. The following is a list of pertinent symbols:

M = mass

T = temperature

E = energy

$\nu$ = normal mode of vibrational frequency of the solid.

$\Omega_\nu$ = modal frequency

$\Theta$ = characteristic temperature of solid

$\Omega_{max}$ = maximum of modal frequencies.

$\hbar\Omega_{max} = k\Theta$ defines the characteristic solid temperature. A set of dimensionless variables is used, as defined by the following relationships:

$\tau$ = time = $\Omega_{max}t$ (t = real time)

$\omega_\nu = \frac{\Omega_\nu}{\Omega_{max}}$

$\varepsilon = \frac{E}{k\Theta}$

$v = \frac{V}{k\Theta}$

$\delta = \frac{\Delta}{k\Theta}$

$l = aL$

$Z = az$

$t = \frac{T}{\Theta}$ (dimensionless temperature)

$m = \frac{Mk\Theta}{\hbar^2 a^2}$

Six dimensionless parameters are necessary to describe the transition probability between an arbitrary initial and final state of the gas-surface system. They are $\mu = m_g/m_s$, $m_g$, $\varepsilon_{gi}$, $\varepsilon_{gf}$, $t_s$ and d where

$d = (2m_g\delta)^{1/2}$.

The initial state of the system is $|gsi\rangle$, while the final state is $|gsf\rangle$. The probability per unit time of transition between the initial and final state is

$$P(gsf, gsi) = 2\pi|\langle gsf|v|gsi\rangle|^2\ \delta(\varepsilon_{gsf} - \varepsilon_{gsi}) \tag{4}$$

The potential is expanded as a power series and the gas-surface state is separated into a state for the gas and a state for the solid. The probability now becomes

$$P(gsf, gsi) = 2\pi|\langle sf|Z_s|si\rangle|^2\ |\langle gf|v'|gi\rangle|^2 \times \delta(\varepsilon_{sf} + \varepsilon_{gf} - \varepsilon_{si} - \varepsilon_{gi}) \tag{5}$$

The problem is now reduced to determining the two matrix elements for the transition. The matrix element $\langle sf|Z_s|si\rangle$ is evaluated by writing $Z_s$ in terms of annihilation and creation operators for phonons in the solid and $|s\rangle$ is expanded in the phonon eigenstates. After making a thermal average over the phonon modes the matrix element becomes

$$\frac{3\mu}{2m_g}\left[\frac{(\varepsilon_{gf} - \varepsilon_{gi})\ I\ (|\varepsilon_{gf} - \varepsilon_{gi}|)}{\exp\ ((\varepsilon_{gf} - \varepsilon_{gi})/t_s) - 1}\right] \tag{6}$$

where $I(x) = 1 \quad 0 < x < 1$

$= 0 \quad 1 < x < 0$

In order to agree with the nomenclature used in more recent quantum treatments,[34] an A matrix is defined as

$$\langle gf|A|gi\rangle = m_g\left(\frac{1}{(p_{gf}\ p_{gi})^{1/2}}\right)\langle gf|v'|gi\rangle \tag{7}$$

where $p_{gf}$ is the final gas momentum. Matrix elements for the Morse

potential used by Lennard-Jones, Devonshire and Strachan are given by[35]

$$(8)\quad |\langle gf|A|gi\rangle|^2 = \pi^2 \frac{\sinh(2\pi p_{gf})\,\sinh(2\pi p_{gi})}{[\cosh(2\pi p_{gf}) - \cosh(2\pi p_{gi})]^2} (p_{gf}^2 - p_{gi}^2)^2 \times \left[\left|\frac{\Gamma(1/2 - d + ip_{gf})}{\Gamma(1/2 - d + ip_{gi})}\right| + \left|\frac{\Gamma(1/2 - d + ip_{gi})}{\Gamma(1/2 - d + ip_{gf})}\right|\right]^2$$

The transition probability can now be calculated in terms of the system parameters described above.

Since this is a first order perturbation theory, it is expected to be valid near the classical limit where $\mu$ is small and the gas-solid energy transfer is small. As the energy transferred increases, and as the probability of one phonon encounters decreases, this first order treatment no longer holds.

An obvious improvement to this theory would be to extend it to three dimensions. Also a theory based on conservation of particle flux would eliminate the problem of multiphonon encounters. Some account should also be taken of the presence of surface phonon modes. Efforts along these lines have been undertaken and will be discussed briefly in the section on quantum mechanical treatments. These early quantum theories have offered insight into the microscopic details of the gas-surface energy exchange. The next section deals with some simple classical theories which have also helped in this regard.

C. Cube Theories

Perhaps the most widely applied theory of the scattering of gas atoms from a solid surface is the so-called hard cube model of Logan and Stickney[36] and its derivatives. The success of these theories is based on their simplicity and their ability to predict qualitatively the scattering distributions for a wide variety of gas-solid sytems. The basic assumptions, results, successes, and shortcomings of the hard cube theory will be discussed in what follows. The soft cube theory[37] and some recent extensions[38,39] will be treated as well.

The hard cube model is based on four assumptions. These assumptions are:[36,40,41]

(1) The gas particle and the surface atom are rigid elastic particles.

(2) The surface is perfectly smooth. This means that the tangential component of the gas particle velocity is not changed on collision with the surface.

(3) The surface atoms are independent particles confined by square well potentials.

(4) A one-dimensional Maxwellian distribution of velocities is chosen for the motion of the surface atoms normal to the surface.

A schematic diagram of the model is shown in Figure 4.

The analysis of the hard cube model followed three paths initially. In the first case,[36] the initial speeds of the gas particle and surface atom are given by mean speeds. The derivation is restricted to gas atom/surface atom mass ratios ($\mu$) of $<1/3$ and gives a closed form

solution for the position of the scattering pattern maximum only. The resulting expression for the position of the scattering distribution maximum is:

$$(9) \qquad \eta = \theta_0 - \cot^{-1}\left[\cot\theta_0 \left(\frac{1-\mu}{1+\mu} + \frac{16}{9\pi}\frac{\mu}{1+\mu}\frac{T_s}{T_g}\frac{1}{\cos^2\theta_0}\right)\right]$$

where

$\theta_0$ = angle of incidence

$\theta_1$ = angle of reflection

$\eta = \theta_0 - \theta_1$

$T_s$ = surface temperature

$T_g$ = gas temperature

} define the mean speeds of the surface atom and gas atom velocity distributions.

The second analysis of the model[36] results in an expression for the entire scattering distribution, but requires numerical integration. It takes into account the distribution of velocities of both the surface atom and the incident gas particle. The result of this analysis is the expression below:

$$(10) \quad F_1(\theta_1, \theta_0, m_g, T_g, m_s, T_s) = \frac{1+\cot^2\theta_1}{\cot\theta_0}\int_{u_{n0}=0}^{u_{n0}=\infty} F_0(u_{n0}, \theta_0, m_g, T_g) \times$$

$$F_1(u_{n1}, u_{n0}, \theta_0, m_g, m_s, T_s)\, u_{n0}\, du_{n0}$$

where $u_{n0}$ and $u_{n1}$ are the normal components of the gas particle velcoity before and after scattering.

The third analysis[40,42] results in a closed form expression for the complete scattering distribution and for the velocity distribution of the scattered particles. By making the further assumption that multiple collisions of the incident particle with the surface are unimportant,

equation 11 for the scattering probability of a flux of gas particles into a unit angular range $d\theta_1$ at angle $\theta_1$ results.

$$(11) \quad P(\theta_1) = \frac{3}{4}\left(\frac{m_s T_g}{m_g T_s}\right)^{1/2} B_2(1 + B_1 \sec\theta_0) \left(1 + \frac{m_s T_g}{m_g T_s} B_1^2\right)^{-5/2}$$

$$\text{where (11a)} \quad B_1 \equiv \left(\frac{1+\mu}{2} \sin\theta_0 \cot\theta_1 - \frac{1-\mu}{2} \cos\theta_0\right)$$

$$\text{where (11b)} \quad B_2 \equiv \left(\frac{1+\mu}{2} \sin\theta_0 \csc^2\theta_1\right)$$

Employing a similar analysis for the calculation of the velocity distribution of the particles at each $\theta_1$ gives an expression for the velocity distribution of the atom flux leaving the surface at any angle $\theta_1$. This expression is:

$$(12) \quad P(U) = 2B_3^4 \left(1 + \frac{m_s T_g}{m_g T_s} B_1^2\right)^2 U^3 \exp\left[-B_3^2\left(1 + \frac{m_s T_g}{m_g T_s} B_1^2\right) U^2\right]$$

U is the dimensionless velocity defined by

$$(13) \quad U = u_1\left(\frac{m_g}{2kT_g}\right)^{1/2} \quad \text{and}$$

$$B_3 \equiv \frac{\sin\theta_1}{\sin\theta_0}$$

The results of these analyses can be concisely stated by examining the behavior of the deviation of $\theta_1^{max}$ from specular ($\eta$) as a function of the system parameters, and comparing this behavior with the experimental behavior.

| Hard cube prediction | Experimental results |
|---|---|
| $\frac{\partial \eta}{\partial m_g} > 0$ | $\frac{\partial \eta}{\partial m_g} > 0$ |
| $\frac{\partial \eta}{\partial T_s} > 0$ | $\frac{\partial \eta}{\partial T_s} > 0$ |
| $\frac{\partial \eta}{\partial T_g} < 0$ | $\frac{\partial \eta}{\partial T_g} < 0$ |
| $\frac{\partial \eta}{\partial \theta} \lesseqgtr 0$ | $\frac{\partial \eta}{\partial \theta} \lesseqgtr 0$ |

Figure 5 shows experimental and theoretical scattering distributions for comparison.

The remarkable qualitative agreement between this model and the observed scattering behavior indicates that the assumptions upon which the model is based are valid assumptions to a first approximation. Stickney[41] and Logan et al.[40] discuss the assumptions in detail and suggest modifications which have been incorporated in the theory. Goodman[43] has indicated a quantum mechanical basis for the assumption of a planar equipotential surface. The assumption of a planar equipotential surface and the experimental evidence supporting this assumption say a great deal about the nature of energy trnasfer in the gas-solid interaction. To a first approximation, change in tangential momentum can be ignored in the scattering of gas particles from a solid surface. Of course, at grazing angles of incidence, or where chemical reaction takes place, the approximation breaks down. In any case, this assumption, and the hard cube theory based upon it, have added significantly to our understanding of gas-surface energy transfer.

Several of the drawbacks of the hard cube model have led to modifications and extensions of the theory to include more physically realistic assumptions. In most cases, these extensions have also led to a more complex theory requiring numerical solution. The first important revision of the model by Logan and Keck is termed the soft-cube model.[37] As its name implies, the gas-solid potential is assumed to be made up of a square well attractive potential resulting in a "soft" gas-surface collision and an exponential repulsive potential. (Figure 6.) The attractive potential is assumed fixed in space while the repulsive part of the potential oscillates about the equilibrium position of the surface atom which behaves as if attached to the remainder of the rigid lattice by a single spring. The result of the analysis for in plane scattering is given by equation 14:

$$(14) \qquad P(\theta_1) = \left(\frac{m_s u^2}{2\pi k T_s}\right)^{1/2} (1 - v_c) \left|\frac{dv_i}{d\theta_1}\right| \exp\left(-\frac{m_s u^2 v_i^2}{2kT_s}\right)$$

where $u$ = incident normal velocity inside potential well

$v_c = (v \cos\omega t_0)/u$

$v_i$ = initial amplitude of the surface oscillator

$t_0$ = time of turning point in collision

The soft cube model in this form introduces three parameters to describe the potential; the well depth D, the interaction range b, and the surface atom oscillator frequency $\omega$. These parameters are reflected in the final result by u, v and $t_0$. Forman,[38] and Karamcheti and Scott[44] have utilized a truncated harmonic potential in the soft cube model which simplifies the analysis somewhat. The soft cube model also allows consideration of

those particles which are trapped upon collision with the surface. The soft cube model predicts the same trends of experimental parameters as the hard cube model, but greatly improves the quantitative agreement with experiment, especially in the case of the scattering distribution width.

A recent extension of the cube theories is that by Doll.[39] He has developed the formulism to include scattering of a rigid rotor by the surface. This extension has improved the agreement of theory and experiment for the scattering of diatomic molecules from solid surfaces, particularly the widths of the scattering distributions. A comparison of experimental results with the simple hard cube model and the modified rigid rotor model is shown in Table I. Figure 7 shows the collision geometry of this modified model. The final result for the scattering distribution is given by equation 15.

$$(15) \qquad P(\theta_1) = \frac{2}{\pi^2}\left(\frac{\mu_T}{\mu_m}\right)^{1/2}\left(\frac{1 + \mathrm{ctn}^2\theta_1}{\mathrm{ctn}\theta_0}\right)\cos\theta_0 \times$$

$$\int_0^{\pi/2} \frac{(1 + \mu_m + S^2)(1 + \gamma)\, d\phi}{[1 + (\mu_T/\mu_m)S^2]^{1/2}\left\{1 + (\mu_T/\mu_m)\cos^2\theta_0\gamma^2/[1 + (\mu_T/\mu_m)S^2]\right\}^2}$$

where:

$$\mu_T \equiv \frac{T_g}{T_s} \qquad \mu_m \equiv \frac{m_g}{m_s} \qquad S \equiv \sin\phi$$

$$\gamma \equiv 0.5[(1 + S^2 + \mu_m)(\mathrm{ctn}\theta_1/\mathrm{ctn}\theta_0) + \mu_m + S^2 - 1]$$

Replacing $\sin\phi$ by zero gives the correct two-dimensional atom/hard cube expression[36,39] as would be expected.

TABLE I. Shown are the experimental (E), atom/hard cube (HC), and modified rigid rotor (MRR) maxima locations ($\theta_{max}$) and widths (fwhm) for several diatomic scattering distributions. Tg and Ts give beam and surface temperature (°K) and FRR is $2\phi_{max}/\pi$. (Ref. 39.)

| | | | | | $\theta_{max}$ | | | fwhm | | |
|---|---|---|---|---|---|---|---|---|---|---|
| System | Tg | Ts | $\theta_i$ | FRR | E | HC | MRR | E | HC | MRR |
| $D_2$ + Ag | 80 | 560 | 50 | 0.68 | 41 | 33 | 33 | 49 | 38 | 42 |
| $D_2$ + Ag | 300 | 560 | 50 | 0.39 | 51 | 46 | 46 | 31 | 28 | 32 |
| $D_2$ + Ag | 1400 | 560 | 50 | 0.19 | 53 | 51 | 51 | 15 | 14 | 15 |
| $D_2$ + Ag | 80 | 560 | 70 | 0.68 | 47 | 45 | 43 | 51 | 54 | 56 |
| $D_2$ + Ag | 300 | 560 | 70 | 0.39 | 64 | 64 | 62 | 39 | 35 | 40 |
| $D_2$ + Ag | 1400 | 560 | 70 | 0.19 | 69 | 70 | 69 | 18 | 16 | 18 |
| $H_2$ + Ag | 300 | 560 | 50 | 0.28 | 50 | 48 | 48 | 5 | 20 | 23 |
| $N_2$ + Ag | 300 | 600 | 50 | 0.83 | 48 | 31 | 32 | 42 | 48 | 52 |
| $N_2$ + Ag | 1500 | 600 | 50 | 0.46 | 55 | 56 | 55 | 25 | 37 | 43 |
| $N_2$ + Pt | 300 | 475 | 45 | 0.83 | 43 | 36 | 36 | 48 | 39 | 46 |
| $N_2$ + Pt | 298 | 521 | 45 | 0.83 | 44 | 35 | 35 | 48 | 40 | 45 |
| $N_2$ + Pt | 298 | 800 | 45 | 0.83 | 34 | 29 | 29 | 48 | 39 | 43 |
| $N_2$ + Pt | 298 | 973 | 45 | 0.83 | 32 | 26 | 27 | 48 | 38 | 42 |
| $O_2$ + Pt | 300 | 475 | 45 | 0.86 | 45 | 36 | 35 | 51 | 41 | 47 |
| $H_2$ + Pt | 300 | 1175 | 45 | 0.28 | 44 | 42 | 42 | ~60 | 20 | 22 |
| $D_2$ + Pt | 300 | 1175 | 45 | 0.39 | 45 | 40 | 39 | ~60 | 26 | 30 |

The success of the "cube" theories in explaining and predicting gas-surface scattering distributions has added a great deal to the understanding of the gas-solid energy exchange. The simplicity of the results and the apparent experimental verification of many of the assumptions upon which the theories are based has led to a physical picture of the processes involved in the gas-surface interaction.

D. Classical Scattering Theory

Brief mention will be made of the classical trajectory type calculations of gas surface scattering. Extensive references to the original literature are included for the reader interested in examining these theories in greater detail. Effectively, three groups have developed this method in the past decade. The method consists of numerical solution of the equations of motion for a large number of gas particles incident on an idealized surface. The surface is composed of a lattice of atoms connected by harmonic potentials. The approaches of the three groups differ in numerical techniques and the gas-surface interaction potential used in the calculation.

Lorenzen and Raff[45-49] utilize a Morse potential for the interaction. Calculations for two-[45] and three-[46] dimensional surfaces exhibit semi-quantitative agreement with experimental data for He scattering from Ni and Ar from W.[49] They treat the effect of surface impurities,[47] finding an increase in energy transfer for surfaces contaminated by submonolayer quantities of contaminants.

McClure[50-53] uses a 6-12 pairwise interaction potential. His two-dimensional finite range interaction model points out the dependence of the scattering results on the tangential momentum transfer.[50] This dependence is neglected in the cube models discussed previously. A very interesting result of these calculations is the appearance of "surface rainbows"† in the calculated scattering distribution.[51] This structure

† So named because of similarities between this effect and rainbow structure observed in gas phase scattering. For example, see H. C. Van de Hulst, Light Scattering by Small Particles (J. Wiley & Sons, New York, 1957).

can be used to extract information about the gas-surface interaction potential. Comparisons are made with experimental data for Ne/LiF scattering showing very good quantitative agreement.[52,53]

The calculations of Oman[54-59] use a 6-12 potential for the gas-surface interaction. The theory is three-dimensional and has been applied to the scattering of rare gases[54,59] and diatomic molecules[56] from silver. Qualitative agreement with experiment and the simple cube theories is obtained. The calculations also agree with the hard sphere model of Goodman[60-62] at the limit of high incident gas energy.

Several other trajectory type calculations have been done,[63-65] but all attempts suffer from the same drawback. The convergence characteristics of the Monte Carlo techniques used necessitate the calculation of $10^4$ to $10^5$ trajectories for each set of incident conditions. This is an expensive way to extract information about the gas-surface potential field. Recent work by Steele[66,67] giving an analytical expression for the scattering probability, and the semiclassical methods developed by Doll[68,69] and others, appear to give a large return of information for invested computational time.

E. Quantum Mechanical Theories

Present day quantum mechanical treatments of gas-surface energy exchange have built on the early theory of Lennard-Jones, Devonshire and Strachan.[31-33] As discussed above, the major problems of the early theory were that it was one-dimensional, it could not account for large non-specular fluxes (first-order perturbation theory), it treated surface atoms as if in the bulk, and the inelastic scattering theory was limited to single phonon processes. Recent developments in the theory have attempted to correct these problems. An extensive review of the state of quantum theories of scattering up to 1966 is given by Beder.[70] More recent reviews by Goodman[35,71] discuss several of the corrections.

A revival of interest in quantum theories of gas-surface scattering in the mid-1960's stimulated the work of Beder,[72] Howsmon[73] and Tsuchida.[74] Their work, as well as the early efforts of Goodman and coworkers[34,75] extended and clarified the one-dimensional single phonon first order theory of Lennard-Jones and Devonshire.

The breakdown of the first order perturbation treatment was discussed initially by Cabrera, Celli, Goodman, and Manson.[34] They developed first an elastic scattering theory and then a one phonon inelastic theory[76] which is based on the conservation of particle flux (an unitary theory).[75] The elastic theory has been applied with qualitative success to the scattering of $^{3}He$ and $^{4}He$ by LiF.[75] The role of various attractive potentials in the framework of this theory has been investigated by Goodman.[77,78]

Beeby's development of a formalism to treat multiphonon encounters[79-81] indicates that one and even two phonon terms do not explain experimental results. The numerical calculation required to deal with multiphonon scattering is so extensive that infinite order calculations are not feasible. His treatment depends on the Debye-Waller factor for explanation of observed diffraction. Weinberg[82] points out that local surface potential is just as important in this regard.

The problem of generalization to three dimensions and recognition that the surface atom is not in fact like an atom in the bulk of the solid was treated by Goodman.[83] The surface atom is assumed to behave as if its characteristic temperature were that of the surface Debye temperature[84] rather than the bulk Debye temperature. This theory is extended to be generally applicable in the treatment of elastic and inelastic scattering separately and in combination.[85-87] The inelastic theory is able to predict phonon creation and annihilation peaks around elastic scattering peaks.

The quantum theory of gas-surface scattering has progressed to the stage where qualitative agreement with experimental results is generally obtained. Very recent treatments are yielding quantitative agreement for helium/alkali halide scattering systems. Since a detailed theoretical understanding of the gas metal energy transfer is essential to an understanding of heterogeneous catalysis, this field will remain a fruitful one for theoretical study.

F. Reactive Scattering Theory

There has been very little work on the development of theories for reactive gas-surface scattering. What work has been done has generally been limited to model descriptions of particular experimental systems.[88-91] There have been few attempts at formulating a general theory of reactive scattering. For the most part, this can be explained by the variety of processes that constitute reactive scattering and which a general theory should be able to treat. These processes are:

(1) Dissociation or rearrangement of the incident gas particle on collision with the surface. $AB_{gas} \rightarrow A_{surf} + B_{surf}$

(2) Formation of chemical bonds between incident and surface atoms on impact. $A_{gas} + B_{solid} \rightarrow AB_{gas}$ or $AB_{surf}$

(3) Reaction of incident particles with other particles from the gas phase at the surface or with atoms adsorbed on the surface.

$A_{surf} + B_{surf} \rightarrow AB_{surf}$ or $AB_{gas}$

(4) Desorption of volatile surface species containing atoms of the surface or only atoms from the gas phase. $AB_{surf} \rightarrow A_{gas}$ or $AB_{gas}$

These various processes occur separately or simultaneously during reactions such as dissociative chemisorption, oxidation, heterogeneous catalysis and vaporization. An interesting discussion of the energetics, possible mechanisms and kinematics of these processes is given by Wise and Wood[92] in their review article on reactive collisions between gas and surface atoms.

Lacking a general theoretical treatment of reactive scattering, the various processes making up reactive scattering have been investigated.

Theoretical treatments of dissociative chemisorption[93-97] and surface ionization[98,99] are available. Macroscopic theories of oxidation and oxide scale growth are well known.[100] Theories of heterogeneous catalysis are less numerous because this again involves several separate processes, but there are electronic[101,102] and geometric[103,104] arguments proposed to explain catalytic behavior. The Langmuir-Hinshelwood[105] mechanism and the Rideal-Eley[106] mechanism have been used to explain catalytic systems for several years. Batty and Stickney,[107] and Weber and Cassuto[108] have used quasi-equilibrium thermodynamics to expalin evaporation rates of volatile transition metal oxides at low pressure and high temperature.

In general, reactive scattering theories take their form from several fields not necessarily related to molecular beam scattering from solid surfaces. In the future, it is hoped that more cohesive theories will be available which build on the energy exchange foundation of the scattering theories described previously and incorporate the results of much work in the fields of chemisorption, oxidation, catalysis and vaporization.

## 3. Experimental Techniques

### A. The Molecular Beam Surface Scattering Experiment

As mentioned previously, molecular beam techniques are particularly well suited to the study of the gas-solid energy exchange. The reason for this suitability lies in the ability to characterize with a fair degree of certainty the initial and final states of the gas. Molecular beam methods can provide a spatially defined incident flux of gas particles with a given kinetic energy or distribution of kinetic energies.[1] The internal energy of the gas can be selected using proper techniques.[109] Particles leaving the solid can be characterized as to composition, direction, and energy (both translational and internal). When these techniques are combined with modern methods of solid surface preparation and characterization, a very powerful tool is available to the experimenter interested in the gas-solid energy exchange.

The preparation of well characterized solid surfaces has depended greatly on the development of the technology for attaining and maintaining ultra high vacuum ($<10^{-9}$ Torr Hg).[110] Only in an ambient atmosphere of this magnitude can a surface be expected to remain free of contaminants from the background for periods of time long enough for surface studies.[84] The study of atomically clean surfaces can be accomplished in the folowing three ways.[111] (1) Ideally, a clean surface is prepared by *in situ* methods (cleaving, chemical treatment, ion bombardment) and is kept clean by performing the studies in UHV.[112] (2) The surface of a refractory metal sample (such as tungsten or tantalum) is cleaned by

heating to a high temperature and is kept clean by keeping the surface so hot that contaminants will not stick.[113] (3) The solid surface is kept clean by continuous deposition of the surface layer at a rate greater than the flux of contaminants from the background gas.[114] The actual preparation of atomically clean solid surfaces for molecular beam scattering targets often combines these three techniques to some extent.

Once a clean surface has been prepared, the condition of the surface must be characterized. This can be accomplished in several ways. The use of high purity bulk single crystal samples is very helpful in providing a surface with definable atomic geometry.[112,114,115] This geometry can be verified by the technique of Low Energy Electron Diffraction (LEED).[116] The chemical composition of the target surface must also be known. This can be determined by electron spectroscopy of the first few atomic layers of the sample. Two techniques in particular are especially sensitive to the chemical composition of the surface. These are Auger Electron Spectroscopy (AES)[117] and ultraviolet or x-ray photoelectron spectroscopy (UPS and XPS).[118] The combination of modern surface analysis tools like LEED and AES with ultra high vacuum techniques for molecular beam scattering studies have provided a large source of solid experimental information on the details of the gas-solid interaction. Several research groups are at present using systems designed with the above considerations in mind,[112,115,119] and much more information about beam scattering from well defined solid surfaces is forthcoming. Figure 8 shows a schematic diagram of a scattering apparatus designed for well characterized surface work.

B. Sources

The production of a high intensity well collimated atomic or molecular beam is crucial to the study of gas-solid energy exchange by molecular beam techniques. An ideal source for such an experiment must satisfy several criteria. (1) It must be of a high enough intensity that useable signal-to-noise ratios are obtained. (2) It should be monoenergetic or at least have a well defined energy distribution. (3) It must be spatially defined with small divergence, so that the angle of collision is well known. (4) It should be of variable intensity, variable energy, and it should be versatile (a range of molecules and atoms able to be used).

There are three basic source configurations which meet these criteria to a greater or lesser extent and involve varying amounts of technical investment. These source configurations are the effusion source, the multichannel capillary array, and the nozzle beam source. Figure 9 shows a schematic diagram of the three sources along with their angular distribution and velocity distribution characteristics.

The effusion source is generally a temperature controlled oven with a small opening through which the source gas effuses randomly. The laws governing effusion are well known and are treated in any standard textbook on physical chemistry,[120] the major requirement being that the mean free path of the gas inside the source must be greater than the oven orifice. The angular distribution of molecules emerging from the opening varies as the cosine of the angle from the normal to the source opening. The energy distribution of the molecules is a Maxwellian distribution at the temperature of the oven. The advantages of this source are its simplicity and well

defined beam energy distribution. Since it must be operated at pressures low enough that the effusion is random, its major drawback is its low intensity.

The multichannel capillary array is basically an effusion oven fitted with a small opening composed of a bundle of very fine capillary tubes. Figure 10 shows a photomicrograph of such an array. The length-to-diameter ratio of these tubes is of the order of 50 to 1, resulting in a source whose angular distribution is peaked along the normal to the source opening. In this way, higher intensities are attained at the target for the same total leak rate and therefore the same investment in pumping speed. These sources can also be operated at pressures above those for random effusion, again increasing the source intensity. The energy distribution of the beam molecules is experimentally determined to be nearly Maxwellian, with a slight increase in high speed molecules at the expense of the low energy tail of the distribution. A series of papers by Olander and coworkers[121-127] treats the design, use, and theoretical aspects of these very useful molecular beam sources.

The supersonic nozzle source is used to produce very high intensity nearly monoenergetic molecular beams. Free expansion of a high pressure gas through a nozzle-skimmer arrangement converts the enthalpy of the gas into a net translational energy along the normal to the nozzle opening.[128] This expansion produces a cooled beam whose translational speed is determined by the nozzle-skimmer geometry but whose speed distribution can be characteristic of very low temperature. This narrow distribution and the fact that rotational and vibrational temperatures can be defined for the expanded gas make this source very useful when the energy of the incident molecular beam must

be well known. Its ability to operate at very high driving pressures gives a high intensity beam but also provides its major shortcoming. Very large pumping speeds are required to pump away the high throughput of molecules. Using seeding techniques,[129] nozzle beam sources can attain energies from less than .1 to about 20 eV. The original work of Kantrowitz and Grey,[130] and of Kistiakowsky and Schlichter[131] as well as several review articles,[129,132,133] discuss the design and use of nozzle beam sources.

The problem of producing a monoenergetic source without the large pumping requirements of the nozzle source can be solved with the use of a slotted disk velocity selector.[134] A series of slotted wheels are placed in the molecular beam produced by an effusion type source. (Figure 11.) By proper placement of the openings and rotation of the assembly at constant speed, only a certain portion of the velocity distribution can pass through the filter. This results in a nearly monoenergetic beam at the loss of a great deal (about 99% usually) of the incident beam intensity.

There is a great deal of literature available on the design of specialized sources such as sources for ions or dissociated atoms. This literature is reviewed in the standard works on molecular beam techniques such as Ramsey[1] and Fraser[135] as well as the annual series on advances in chemistry and physics.[136]

C. Detectors

The detection of particles leaving the surface can be accomplished in several ways. Surface ionization detectors are useful for alkali and alkaline earth atom scattering from surfaces. Their high sensitivity for these species is offset by the very narrow range of species which they will detect. Very little surface scattering is done using alkali atom beams, so the use of this detector in gas-surface scattering studies is not widespread.[137]

A more versatile detector is one based on the ionization of particles to be detected by interaction with an electron beam. These electron bombardment detectors fall into two general categories; ion gauges and mass filters. As Figure 12 shows, the ion gauge measures a total ion current while the mass filter measures a signal due to a particular mass ion.

The most widely used mass filter detector is the compact quadrupole mass filter. Figure 13 shows a schematic diagram of a typical quadrupole detector. Ions are formed in the ionizer by bombardment with ~70 eV electrons. The ions are extracted downward through the quadrupole assembly which defines a variable RF-DC field. Ions of the proper mass to charge ratio for the particular field pass through the filter and strike an electron multiplier or Faraday cup collector where the current due to that ion is measured. All other ions have unstable trajectories in the RF-DC field and collide with the quadrupole assembly instead of being detected. The advantages of the mass filter and ion gauge detectors are their universal applicability. However ionization is inefficient with one ion produced for every $10^4$ - $10^5$ particles passing through the detector. The mass filter

detector is essential when reactive scattering takes place and the identity of particles leaving the surface must be known.

Figure 12 also indicates the difference between a flux sensitive and density sensitive detector. The signal from the flux sensitive detector is proportional to the total flux entering the detector, since there is only one opening to the detector. The density sensitive detector produces a signal proportional to the instantaneous number density of particles in the ionizing region, since the particles are allowed to flow through the ionizing region.[111,138]

Detectors for gas-surface scattering can be either fixed or rotatable about the crystal surface. Fixed detectors are generally used only in systems designed to study reactive scattering.[139] The techniques used to study reactive scattering will be discussed in a later section. Rotatable detectors present a design problem of fair proportions in an ultra-high vacuum scattering chamber.[112] They are however absolutely essential for elucidation of the nature of gas-surface energy exchange, because of the information available in the angular distribution. Both ion gauge[140] and mass filter detectors[112,139] have been successfully incorporated in ultra high vacuum scattering systems.

A word or two should be said here about the use of lock in detection to improve the signal to noise characteristics of gas-surface scattering systems.[141] Generally the incident molecular beam is mechanically chopped at a fixed or variable frequency and the scattered signal is detected and amplified by a narrow band amplifier tuned to the same frequency. See Figure 14. This eliminates detection of gases not modulated at the incident beam frequency and improves signal to noise

ratios by several orders of magnitude. More will be said about this useful technique in the section on reactive scattering methods.

## D. Velocity Measurement

Important complementary information to the angular scattering distribution determined with rotatable detectors is the velocity distribution of particles leaving the surface. This information is essential to a complete understanding of the gas-surface energy exchange,but unfortunately it is not without experimental difficulties.

The most straightforward method of determining the velocity distribution of the scattered molecules is the use of the slotted disk velocity selector discussed above.[134] The same drawbacks (i.e. loss of signal) apply as when used to monochromatize the incident beam. When used to filter the scattered beam however, further complications arise, the major one being the incompatibility of UHV conditions and the greased bearings of high speed synchronous motors.

Time of flight techniques[137,142-146] can be used to overcome the loss of signal problem. In this case, a single mechanical chopper is used to gate the scattered beam, and delay electronics record the signal in fixed time intervals after the opening of the gate. This technique gives a velocity distribution over a wide range of velocities if the gating frequency can be changed readily. A fixed frequency can give a distribution limited by the particular frequency and the geometry of the detection system. Variable frequency time of flight velocity analyzers are again incompatible with UHV scattering systems, while fixed frequency tuning fork-type choppers are useable in UHV systems.

The average speed of the scattered beam can be easily determined by phase-sensitive detection of the scattered beam at a fixed frequency.[141,147-149] The phase difference between the detected signal and a reference from the chopper is directly related to the time of flight of the scattered molecules. For example, consider a system with a chopper-to-detector distance of 10 cm. If particles traveling from the chopper to the detector have a mean speed of $1 \times 10^5$ cm/sec, the flight time over the 10 cm distance is

$$\tau = \frac{d}{u} = \frac{1 \times 10^1 \text{ cm}}{1 \times 10^5 \text{ cm/sec}} = 1 \times 10^{-4} \text{ sec} \tag{16}$$

If the chopper is operated at $f = 1 \times 10^3$ hz, the phase shift due to flight time will be

$$\begin{aligned} \phi &= (3.6 \times 10^2) f\tau \\ &= (3.6 \times 10^2 \text{ deg /cycle})(1 \times 10^3 \text{ cycles/sec})(1 \times 10^{-4} \text{ sec}) \\ &= 3.6 \times 10^1 \text{ degrees} \end{aligned} \tag{17}$$

In principle, the amplitude of the modulated signal can be used with the phase shift to determine the velocity distribution of the scattered beams.[125] Equation 18 shows the relation between the velocity distribution and the phase and amplitude of the detected signal.

$$f(v) \sim \int_0^\infty I(t) e^{i\omega t} dt = A(\omega) e^{i\phi(\omega)} \tag{18}$$

$f(v)$ is the velocity distribution which is proportional to the integral of the time dependence of the intensity at the detector $[I(t)]$ of a beam chopped with frequency $\omega = 2\pi f$. This integral is the Fourier transform of the amplitude $A(\omega)$ and the phase $\phi(\omega)$ as a function of the angular chopping frequency. This method suffers from the sensitivity of the deconvolution to random experimental errors.

A final method of determining the average speed of particles leaving the surface is based on the difference between a flux sensitive detector and a density sensitive detector.[138] Since the number density signal is proportional to the particle flux divided by the mean particle speed, the ratio of the flux signal to the number density signal should be proportional to the mean particle speed.

$N$ = number density in $cm^{-3}$

$F$ = flux in $(sec^{-1})(cm^{-2})$

$$\frac{F}{N} = \bar{v} \text{ in } (cm)(sec^{-1}) \tag{19}$$

Proper design of a detector that can alternately measure flux and number density signals should give the mean speed.

The techniques for measuring the speed of molecules leaving the solid surface are available, but in each case their experimental incorporation introduces new problems. These problems have so far prevented experimentalists from designing single systems capable of measuring angular and velocity distributions together in a UHV scattering environment. Hopefully work toward this end will be fruitful in the near future.

E. Reactive Scattering Methods

The ability to study the detailed kinetic behavior of surface reactions has been realized due to the development of several experimental techniques amenable to the special problems surface reactions pose. The design and widespread use of compact mass spectrometers, such as the quadrupole mass filter described above, has made detection of reaction product signals routine. Signal processing techniques, such as lock-in detection and ion counting electronics, have become a tool for extracting kinetic information not available by non-molecular beam methods. This section will be devoted to a brief discussion of the principles behind these techniques and their use in unraveling surface reaction mechanisms.

A beam of molecules impinging on a surface with intensity $I_0$, when mechanically chopped at angular frequency $\omega$, can be thought of as a modulated driving function. When a reaction takes place on the surface, this modulated function is changed by the processes of the surface reaction. The surface acts as a differential operator operating on the modulated incident beam. A beam of products leaves the surface with different modulation. By monitoring the waveform of the product modulated beam as a function of incident beam modulation frequency, incident beam intensity, incident beam energy, surface temperature, topography and composition, incident beam angle and scattered beam angle, models for the surface operator (the surface reaction mechanism) can be formulated and compared with the experimental waveform behavior. This is the essence of surface reaction mechanism determination by the modulated molecular beam technique.

Ion counting electronics[150-152] and signal averaging devices can be used to record the entire product waveform. The most detailed information about the surface reaction is contained in the entire waveform, but often the reaction is complex enough to make interpretation of waveform results not entirely unambiguous. A more common technique is to measure only the first Fourier component of the scattered waveform by means of lock-in detection.[149,153] For surface reactions showing first order pressure dependence, the higher order Fourier components do not contain surface reaction information.

The processing of the modulated product beam in the lock-in amplifier (Figure 14) results in a signal with amplitude A, $\phi$ degrees out of phase with the reference signal formed at the mechanical chopper. For first order processes, the behavior of A and $\phi$ as a function of the kinetic variables mentioned above gives information about the surface reaction mechanism. An example of the method for a simple adsorption-desorption process should help to illustrate the technique.[154]

Consider a beam of diatomic molecules $A_2$ of intensity $I_0$ chopped by a gating function g(t). They interact with the surface with sticking probability $\eta$ and desorb with rate constant $k_d$.

$$A_{2(g)} + 2S \xrightarrow{\eta I_0} 2[SA_{ads}] \xrightarrow{k_d} 2S + 2A_{(g)} \tag{20}$$

A surface mass balance on adsorbed A atoms gives

$$\frac{d[SA_{ads}]}{dt} = 2\eta I_0 g(t) - k_d[SA_{ads}] \tag{21}$$

Substituting a sinusoidal driving function for g(t) and a trial solution for $[SA_{ads}]$ gives

$$i\omega[SA_{ads}]^* e^{i\omega t} = 2\eta I_0 g_1 e^{i\omega t} - k_d[SA_{ads}]^* e^{i\omega t} \tag{22}$$

Equation 22 is solved for $[SA_{ads}]^*$ to give

$$[SA_{ads}]^* = \frac{2\eta I_0 g_1}{k_d + i\omega} \tag{23}$$

Writing the complex number in polar form and solving for the rate of desorption ($k_d[SA_{ads}]^*$) gives

$$k_d[SA_{ads}]^* = \frac{2\eta I_0 g_1 e^{-i\tan(\omega/k_d)}}{\sqrt{1 + (\omega/k_d)^2}} \tag{24}$$

A reaction product vector can be defined which is the ratio of scattered product signal to incident reactant flux. In the limit of low reaction probabilities this vector is just the ratio of $k_d[SA_{ads}]^*$ to $I_0 g_1$ modified by a phase factor related to the surface residence time of the products.

$$\tilde{\varepsilon} = \left\{\frac{k_d[SA_{ads}]^*}{I_0 g_1}\right\} e^{-i\phi} = \varepsilon e^{-i\phi} \tag{25}$$

Equation 24 can then be written

$$\varepsilon e^{-i\phi} = \frac{2\eta e^{-i\tan(\omega/k_d)}}{\sqrt{1 + (\omega/k_d)^2}}$$

$\varepsilon$, the ratio of product to reactant signal, is given by

$$\varepsilon = \frac{2\eta}{\sqrt{1 + (\omega/k_d)^2}} \tag{27}$$

and $\phi$, the phase difference between product and reactant signals, is given by

$$\phi = \tan^{-1}(\omega/k_d) \tag{28}$$

By observing the amplitude and phase of the product and reactant signals as a function of chopping frequency $\omega$, $k_d$ can be determined by a plot of $\tan\phi$ *vs.* $\omega$ and $\eta$ can be determined by a plot of $1/\varepsilon^2$ *vs.* $\omega^2$. Determinations of $k_d$ at several surface temperatures can give the activation energy and pre-exponential factor for an Arrhenius-type rate equation. Similar analyses of more complex surface reaction models, including series, parallel and combination series and parallel models, enable the experimenter to extract kinetic parameters and to choose appropriate surface reaction mechanisms.[154]

In the above analysis, a sinusoidal gating function was employed. As has been previously pointed out, for first order surface processes a sinusoidal gating function is allowed in the analysis regardless of the actual waveform of the incident beam due to the lack of information in higher order Fourier components. For processes other than first order the analysis becomes more complex and must take account of the actual gating function waveform. Several examples of non-first order processes have been treated by Olander.[155]

Modulated beam methods can also be used to determine residence times in non-reactive scattering.[156] The phase shift of a modulated beam on scattering from a surface can be directly related to the surface residence time after corrections for beam transit times and instrumental corrections have been made. For example, consider a system with chopper-to-crystal

distance, $d_1$ = 10 cm, and crystal-to-detector distance, $d_2$ = 10 cm. For a chopping frequency of f = $1 \times 10^3$ hz and a beam of particles with average speed u = $1 \times 10^5$ cm/sec, as shown in the previous section, the phase shift due to particle flight time would be

$$(29) \qquad \phi_{flight} = \frac{f(d_1 + d_2)}{u} (3.6 \times 10^2) = \underline{7.2 \times 10^1} \text{ degrees}$$

This would be equal to the measured phase shift if the surface residence time were zero. If a 108 degree phase shift were measured, then

$$(30) \qquad \phi_{res\ time} = \phi_{meas} - \phi_{flight} = 36 \text{ degrees}$$

$$(31) \qquad \tau_{res} = \phi/f(3.6 \times 10^2)$$

$$= \frac{3.6 \times 10^1}{(3.6 \times 10^2)(1 \times 10^3)} = 1 \times 10^{-4} \text{ sec}$$

This simple example should give an idea of the method. In actuality, the fact that a distribution of particle velocities is being dealt with complicates the analysis slightly. Harrison, Hummer, and Fite treat this problem and provide tables of phase shift as a function of distance, particle mass, and velocity for Maxwellian beams.[147]

Cross correlation techniques have also been used to measure the residence time distribution.[157] Care should be exercised in realizing that the phase and amplitude of the scattered beam and their relationship to residence time are somewhat scattering model dependent. Yamamoto and Stickney discuss this point.[158]

## 4. Experimental Studies of Energy Exchange

### A. Diffractive Scattering

The elastic scattering of gas particles from solid surfaces does not involve energy transfer between the surface and the incident gas. The results of elastic scattering experiments do give a great deal of information about the interaction potential between the surface and the gas particle. This information is contained in the presence or absence of diffraction and in the temperature dependence of elastic scattering intensity.

Diffraction of gas particles by a solid surface was first observed by Stern and his coworkers in the early 1930's.[30,158] Their observation of He diffraction by LiF crystals proved the wave-particle duality postulate of the new quantum mechanics. Since that time, the experiment has been repeated with H atoms, $^3He$, $^4He$, $H_2$, $D_2$, and Ne scattered from LiF with well defined diffraction peaks being observed in all cases.[159-167]

Except for the few cases discussed below, diffraction has not been observed on scattering from surfaces other than alkali halide crystals. Tendulkar and Stickney[168] observed well defined diffraction peaks on scattering helium from a tungsten(112) surface. This surface consists of close packed rows separated by troughs as seen in Figure 15. Helium atoms incident perpendicular to the rows showed diffraction, while atoms incident parallel to the rows showed only specular scattering. Weinberg and Merrill[169,170] have observed diffraction of He and $D_2$ from a tungsten carbide surface. This surface was characterized by a stiff WC surface with holes due to stacking faults having the correct periodicity to exhibit a W(110)R(3×5)

LEED pattern. In both cases of diffraction from non-alkali halide surfaces, the diffracting surface had a pronounced periodicity and a stiff solid lattice. For LiF scattering the same conditions are met. As discussed previously, Beeby[79] treats the effect of lattice stiffness as a condition for diffraction. Weinberg[82] points out the necessity for a strongly periodic scattering potential as a diffraction condition. Thus the observation of diffraction from a solid surface tells a good deal about the nature of the gas solid scattering.

The only other reported observation of diffraction from a metal surface has been that of Chappell and Hayward.[171,172] They have reported diffraction from a polycrystalline platinum surface. Since the diffraction was reported at a single angle of incidence and single surface temperature, the observation of diffraction is not well verified. The polycrystalline nature of the surface also suggests scattering from adjacent crystallites could explain the anomolous peak.

Helium diffraction has also been used to detect the ordering of a physisorbed layer of ethanol molecules on a LiF surface.[173] Reorientation of physisorbed ethanol above ~130°K resulted in the observation of diffraction peaks. Below this temperature, and with other organic molecules exhibiting disordered physisorption, no diffraction features were observed. This result again points out the importance of pronounced surface periodicity in diffractive scattering.

Quantitative information about the surface lattice stiffness is contained in the temperature dependence of elastic scattering intensities. In the harmonic oscillator model of the solid,[84] the mean square displacement

of the surface atoms is related to the temperature of the surface by

$$\langle u_z^2 \rangle = \frac{3\hbar^2 T_s}{m_s k \theta_{D\perp}} \tag{32}$$

where $\langle u_z^2 \rangle$ is the mean square displacement, $T_s$ is surface temperature, $m_s$ is surface atom mass, and $\theta_{D\perp}$ is the surface Debye temperature which is characteristic of the lattice stiffness. This surface Debye temperature can be determined by measuring the specular scattering intensity as a function of surface temperature since

$$I_{spec} \alpha \exp\left[-\langle(\Delta \underset{\sim}{k} \cdot \underset{\sim}{u})^2\rangle\right] \tag{33}$$

where $\Delta \underset{\sim}{k}$ is the momentum transfer on impact and $\underset{\sim}{u}$ is the instantaneous displacement of the surface atom. Hoinkes, Nahr and Wilsch[174] determined the surface Debye temperature of LiF to be 568°K by this method.

Doll[266] has treated this problem in more detail. If the gas atom-surface atom well depth is large in relation to the incident gas atom energy, the well depth interaction dominates the scattering. As the ratio of incident energy to well depth increases, the particle is more able to sample the thermal motion of the surface atoms and the classical Debye-Waller attenuation in scattering intensity is observed. This two regime effect is not seen with x-ray and electron scattering because the incident particle energy is much higher than the well depth which is of the order of kT.

Diffractive scattering, although not involving energy transfer between the gas and the surface, gives a great deal of information about the interaction potential between a surface and incident gas atom.

## B. Inelastic Scattering

The greatest wealth of information about the gas-solid energy exchange is contained in the results of inelastic molecular beam scattering experiments. A great number of systems have been studied; some well characterized, others not so well defined. By dealing with the work of the last ten years on two particular systems (silver and lithium fluoride), this section will point out the experimental developments of this period, and the information which has been gained about the nature of the gas-solid interaction. Other systems will be discussed and references given wherever helpful to expand on particular points.

Preparation of well-defined silver scattering surfaces by epitaxial growth on a mica substrate has been used very successfullly by Saltsburg, Palmer and Smith.[175-177] They have determined the scattering distribution for a variety of gases scattered from silver surfaces prepared in this manner. In contrast to their results with gold film[114] the epitaxial silver layers showed very little change in scattering pattern between experiments during deposition and experiments after the film was deposited. The formation of a tightly bound inert contaminated layer with topology similar to the clean surface explains this observation.[175] The contrasting results of the two systems show the importance of the surface layer on the energy exchange with incident gas particles. $NH_3$ was found to scatter with a cosine distribution, indicating complete energy transfer. He, Ne, Ar, Xe and $CH_4$ gave peaked scattering distributions indicating varying degrees of energy transfer. Scattering of velocity filtered

Ar and Xe beams from the silver surface resulted in scattering distributions very similar to those for Maxwellian beams.[176] This indicates that the thermal motion of the scattering lattice is the main reason for the broadness of the scattering patterns and is the most important factor affecting energy exchange in the gas-surface interaction.

The same investigators studied the scattering $H_2$, $D_2$ and HD from the silver epitaxial surface.[177] Their remarkable results are shown in Figure 16. $H_2$ alone shows highly specular scattering characteristic of light atoms such as He or Ne. $D_2$ and HD showed very broadly peaked distributions at much lower intensities. The reason for this difference can be seen by an examination of the nature of internal energy transfer on scattering. The allowed rotational energy transitions of the hydrogenic species are shown in Table II.

Table II - Rotational State Transitions

| | Transition (cal/mole) | | | | |
|---|---|---|---|---|---|
| | J(0-2) | J(1-3) | J(0-1) | J(1-2) | J(2-3) |
| $H_2$ | 1032 | 1720 | | | |
| $D_2$ | 516 | 860 | | | |
| HD | | | 248 | 516 | 775 |

The energy of a Debye phonon in silver is ~450 cal/mole, corresponding rather closely to rotational transitions in $D_2$ and HD. A multiphonon process would be necessary for energy transfer to the internal states of $H_2$. This rotational coupling has been observed on single crystal Ag(111)[178] and at Pt(111)[179] surfaces as well.

Experimental studies of high energy atomic beam scattering from silver surfaces have been made by a number of groups.[180-184] As the incident beam energy is increased, the maximum intensity peak shifts towards the surface tangent. At even higher energies it shifts back again to the normal.[181] This behavior along with theoretical predictions for three models is shown in Figure 17. The study points out the limitations of the cube theories for describing energy exchange for high incident velocity. It also indicates the different parts of the interaction which must be sampled as the incident energy is increased.

The above study, and other investigations, especially work by Miller and Subbarao,[182] and Calia and Oman,[183] indicate a transition between scattering regimes as the incident beam energy is increased. Oman[54,185] characterizes these regimes as thermal scattering and structure scattering. As the incident beam energy is increased, more and more of the surface periodicity is sampled by the atoms, so the beam "sees" the structure of the scattering surface. At thermal energies the interaction is averaged over several lattice sites and the beam is not sensitive to the surface structure. These two regimes call for separate theoretical treatments.

A study of the speed distributions of Ar scattered from single crystal silver surfaces gives direct experimental verification of the nature of energy exchange indicated by cosine and specular scattering. Bishara and Fisher[186] found that thermal energy Ar beams displayed peaked scattering with a large cosine component. Determination of the velocity distribution by time-of-flight techniques indicated nearly Maxwellian distributions with mean speeds near the temperature of the scattering

surface for atoms in the cosine component. Measurements of the velocity in the subspecular lobe indicated tangential momentum conservation and low energy accommodation. A study on Ni yielded similar results.[187] Subbarao and Miller have measured the velocity distributions of high energy Ar beams reflected from Ag.[188] They found constant mean velocity at all scattering angles and nearly Maxwellian velocity distributions much wider than the incident beam velocity spread. This result indicates that the scattering is becoming more elastic, energy transfer being less efficient.

Scattering from silver single crystal surfaces in the thermal regime has been exhaustively studied by Sau and Merrill.[178] They identify three types of scattering in this energy range. He, $H_2$, and $D_2$ exhibit quasi-elastic scattering, characterized by peaked scattering distributions and poor energy exchange. Ne, Ar and Kr show inelastic scattering, as evidenced by broad subspecular distributions which are sensitive to surface temperature. Xe exhibits trapping dominated scattering with a large cosine component and high thermal equilibration. Classification of scattering patterns into these three types correlates well with the reduced gas-surface potential well depth, $D/kT_g$, derived from independent measurements. (D is a Lennard-Jones type well depth, k is the Boltzmann constant, and $T_g$ the characteristic temperature of the incident gas beam.) An interesting correlation with the microscopic roughness of the scattering surface and energy transfer is also noted. As the microscopic roughness is increased in going from Ag(111)[178] to Pt(111)[189] to W(110)[190] to Pt(100),[191] the energy accommodation increases as evidenced by the

broadening and the decrease in intensity of the directed peak.

Before going on to discuss inelastic scattering from LiF surfaces, reference should be made to studies on other metal surfaces which show development similar to that of the silver system.

Platinum[192-196] has also been studied extensively due to its utility in heterogeneous catalysis. Studies of diatomic and polyatomic molecular scattering from platinum as well as other surfaces have shown broader scattering distributions than for atoms of similar mass.[192] The transfer of energy to internal modes is responsible for the more efficient energy exchange. This behavior is supported by recent calculations by Doll.[39] Scattering from graphite,[197,198] nickel,[187,199-203] tungsten,[190,168-170,204] molybdenum,[171,205,206] rhenium,[206,207] and stainless steel surfaces[201] has been studied under varying degrees of characterization. A very interesting study by Siekhaus, Schwarz and Olander[198] of simple gases scattered from graphite indicate that the speed of reflected gas reaches a maximum at a particular surface temperature, dependent on the nature of the gas and surface, and that any increase in surface temperature beyond that point does not change the speed of the reflected gas. Whether or not this is typical of every gas-solid system remains to be seen. The authors do not offer any explanation for this unexpected observation. Clarification of the results of this study could add a great deal to our knowledge of energy transfer.

Several of the studies of beam scattering from LiF have been discussed in the section on diffractive scattering. However several points should be discussed with regard to inelastic scattering in these systems. In general gases heavier than neon do not exhibit diffractive scattering from LiF surfaces. For example, Ar scattered from LiF[208] results in a

broadened subspecular peak as in Ar scattering from metal surfaces. Even with light gases, if internal coupling is possible, diffraction features are broadened and eventually washed out.[160]

Dipole-induced dipole attractive forces have been postulated to explain the observation of Ar scattering peaks in fixed directions along rows of second nearest neighbors in the LiF lattice.[161,209] This observation of fixed peaks purportedly caused by interaction with normal modes of the solid is not describable in terms of the simple cube theories of scattering. Obviously, a viable theory of energy transfer must be able to account for such observations by treating the surface vibrational properties. Calculations by McClure[51] indicate that the fixed scattering peaks have nothing to do with a dipole-induced dipole scattering mechanism. Good agreement is obtained with the results of O'Keefe et al.[210] and the trajectory type calculations of McClure.

Williams[164,165] observes peaks in He and Ne scattering from LiF that can be attributed to phonon emission and absorption in the neighborhood of the elastic peaks. (Figure 18.) Coupled with a useable theory of gas-surface scattering, detailed experiments such as these could be used to determine the surface phonon spectrum of solids. With this information, detailed predictions of energy transfer between the gas and solid can be reliably made.

Selective adsorption in molecular beam scattering from solid surfaces was first observed by Stern.[211] This phenomenon gives information about bound surface states and their energies.[162,163,166,167] A difference in bound state energy is found for the two isotopes of He, while $H_2$ and $D_2$ have comparable but much larger (than He) bound state energies.

It is seen that detailed measurement of inelastic gas surface scattering distributions can give a great deal of information about the nature of energy exchange. Energy accommodation, phonon spectra, and bound state energies are some of the experimental parameters that can be measured and used to describe the energy exchange interaction. In many cases, predictions about energy exchange await a useable, accurate gas-surface scattering theory.

C. Reactive Scattering

The study of surface chemical reactions by molecular beam techniques is the logical goal of gas-surface energy transfer studies. The answer to the question of energy partitioning among the surface atoms and the various degrees of freedom of the desorbing gas particle is vital to an understanding of surface chemistry. More and more work is now being done to elucidate the mechanisms of surface reactions and answer this important question of energy transfer.

Surface reactions fall into two categories; those in which the surface acts as a catalyst for the reaction, and those in which the surface is one of the reactants. The simplest of the first type are surface dissociation, decomposition or rearrangement reactions. More complex examples are hydrogenation, exchange and oxidation reactions. The second type of reactions are exemplified by substrate oxidation and corrosion reactions.

Probably the simplest, yet most important, surface chemical reaction is the dissocation of hydrogen on catalytic surfaces. This reaction is an essential initial step to countless technically important catalytic systems. It has been studied by a variety of techniques on a variety of surfaces,[212] but only recently have molecular beam techniques been brought to bear on this interesting problem. Smith and Fite[213] studied the production of H atoms on scattering $H_2$ from tungsten. Using modulated beam techniques, Krakowski and Olander[113] studied H atom formation on tantalum. Both of these studies indicated an increasing reaction probability with increasing surface temperature and residence times indicating complete thermal accommodation of the atoms before emission from the surface. Mixed hydrogen-

deuterium beams scattered from the tantalum surfaces did not result in HD formation. Surface diffusion and atom evaporation at the high surface temperatures used is thought to account for the lack of HD formation.

Hydrogen-deuterium exchange was observed on scattering deuterium from epitaxial nickel surfaces in an ambient of hydrogen.[214] The angular distribution of the product HD was $\cos^3\theta$, perhaps indicating incomplete energy accommodation. The isotope exchange reaction has also been studied on low and high Miller Index platinum single crystal surfaces. Bernasek et al.[179] have found no HD formation on the Pt(111) surface and 5-10% HD product on scattering from a surface of Miller Index (997) under identical experimental conditions. The (997) surface is composed of low Miller Index terraces of (111) orientation nine atoms wide, separated by steps one atom high. (Figure 19.) Apparently the surface steps are essential to the $H_2$ dissociation and subsequent recombination to form HD. The angular distribution of the HD product was found to be cosine, contrary to the results of Palmer et al.[214] on nickel epitaxial layers. The difference could be ascribed to differences in surface cleanliness or to differences in the HD surface bond caused by the topology of the epitaxially grown surface.[215] Modulated beam studies of the exchange reaction indicate long residence times for the HD product, first order pressure dependence on both $H_2$ and $D_2$ pressure, and a possible two branch mechanism for the dissociation and recombination.[216]

The dissociation of $N_2O$ on catalyst surfaces is a slightly more complicated process. Coltharp et al.[217,218] have used modulated beam techniques to measure the angular distributions of $N_2O$, $N_2$ and NO formed when $N_2O$ is scattered from a polycrystalline tungsten target. Cosine angular

distributions for NO and $N_2$ indicate long residence times for dissociating $N_2O$ molecules. West and Somorjai[89] have obtained similar results for the decomposition of $N_2O$ on clean Pt(100) single crystal surfaces. However, from a carbon covered platinum surface the product angular distribution is peaked near the specular. This indicates direct scattering of the product before thermal equilibration with the surface. The difference can probably be attributed to the exothermicity of reactions between C and $N_2O$ giving CN, CO and $CO_2$ as reaction products. The dissociation of $N_2O$ on the clean surface is an endothermic reaction.

The oxidation of $NH_3$ on platinum, a reaction specific to platinum metals, has been studied by Nutt and Kapur.[219] They find $N_2$, $H_2O$ and NO products formed at the surface and no evidence of a gaseous radical intermediate. As this was a fixed detector apparatus, no information is available on the energy accommodation of the products by angular distribution measurements. A more extensive kinetic study of this important reaction has been undertaken by Ulman and Olander.[220] Preliminary results indicate a pressure dependent sticking probability for $NH_3$.

Smith and Palmer[221] have studied the oxidation of deuterium on an epitaxial platinum surface. They observed formation of $D_2O$ when a modulated $D_2$ beam was scattered from the platinum substrate in an $O_2$ ambient. The angular distribution of the product $D_2O$ was cosine, indicating thermal equilibration with the surface. They propose the mechanism of the oxidation to be the adsorbed state reaction of four D atoms and an $O_2$ molecule to give $2D_2O$. Pressure dependence and angle of incidence dependence measurements support this mechanism.

Several more complex catalytic reactions have been given preliminary examination. The oxidation of ethylene on silver surfaces was found to produce $CO_2$ as the major product by Smith et al.[222] Acharya et al.[223] have studied the isotope exchange and decomposition of water on pyrolytic graphite surfaces. Their kinetic results are explained by diffusion of water into the bulk of the solid target. The decomposition of formic acid on nickel surfaces is presently being studied by Madix and coworkers.[224,225] Preliminary results indicate high sticking coefficients for the reactants and evidence for a surface chain reaction decomposition. Hopefully detailed kinetic studies will be able to shed some light on the energy exchange in this important gas-surface reaction.

Reactions in which the surface plays the role of a reactant have been more extensively studied, perhaps because of the generally higher reaction probability for surface oxidation and corrosion type reactions. McKinley's investigations of the nickel-chlorine[226] and nickel-bromine[227] systems are an early example of this type of study. Results of these studies indicate dissociative adsorption of the halogen followed by desorption of NiX or disproportionation and desorption of $NiX_2$.

The oxidation of silicon and germanium has been extensively studied by molecular beam methods. A reaction probability of ~0.04 was found for the oxidation of germanium and silicon by molecular oxygen.[228-230] Atomic oxygen yielded a reaction probability in the range 0.3-0.6.[231] Oxidation of the semiconductor surface by ozone had a reaction probability of 0.2-0.5.[232] These results indicate that the dissociation of the $O_2$ molecule by transfer of energy from the surface to the oxygen-oxygen bond is the rate limiting step in surface oxidation of these semiconductors.

Similar studies of halogen corrosion of semiconductor surfaces indicated high (0.2-0.5) reaction probabilities for reaction of molecular halogens with the surfaces.[90,233] There appears to be a large steric hindrance to energy transfer between the "dangling bonds" of the semiconductor surface and the oxygen molecule, while the larger halogen molecules and ozone can more easily interact with the surface to form reactive atomic species.

Other oxidation studies have included the oxidation of pyrolytic graphite,[91,234] tungsten,[235] molybdenum,[236] and tantalum.[237] The graphite oxidation appears to be the most complex, with diffusion into the bulk at grain boundaries the rate determining step. Surface diffusion of oxygen to an active site appears to be necessary for the oxidation of molybdenum.

Detailed kinetic studies of surface reactions by molecular beam techniques are adding a great deal of information to the surface scientist's knowledge of energy transfer in the gas-surface interaction. More work needs to be done in determining the dependence of reaction rates on the energy state of the gas particle, and on determining the partitioning of energy among the reaction products. This information, along with kinetic parameters for a wide variety of reactive systems, will hasten the understanding of such processes as catalysis and corrosion.

D. Other Methods

A great deal of information about the gas-surface energy exchange is available from molecular beam type experiments which do not readily fall into the classifications discussed above. Microbalance momentum transfer studies, condensation, and desorption experiments all give important information about the energy transfer process.

The use of a microbalance to measure directly the force of an incident beam of molecules on a solid surface can give information about the normal momentum transfer in the gas-surface interaction. Early work by Stickney[238] indicated an increase in the efficiency of momentum transfer with increasing incident gas molecular weight and roughness of the target surface. Under the non-UHV conditions of the experiment, the accommodation appeared to be independent of the nature of the solid itself. These results cannot be explained by assuming a specularly scattered component and a completely accommodated cosine component. Abauf and Marsden[239] have studied the angular dependence of momentum accommodation with a similar experimental apparatus. By extrapolation they derived values for the normal momentum accommodation of He and Ar on contaminated Al and mica surfaces for various incident beam energies.

The deposition of molecules on a surface from a molecular beam can be used with a variety of other techniques to learn about energy transfer. The deposition of atomic and molecular $H_2$ on a tungsten field emitter tip[240] indicates that the condensation depends on a critical velocity of the $H_2$ molecule for the second adlayer. The first layer has a sticking coefficient independent of the incident $H_2$ velocity. Reflection coefficients for atomic

oxygen have been measured with a pulsed beam method on a variety of surfaces.[241] The reflection coefficient is found to be strongly temperature dependent, particularly for metal surfaces. Direct measurement of sticking coefficient (or fraction trapped) can be accomplished with a molecular beam technique. Accurate knowledge of the incident flux in the molecular beam and the pressure in the chamber enable accurate measurement of the sticking probability. For $N_2$ on W foil $S_0$ was found to be 0.61 ± 0.02 independent of angle of incidence.[242] The initial sticking probability on W(111) was found to be 0.08 ± 0.01 and on W(110) no adsorption was detected. This again points out the importance of grain boundaries and step and edge sites for chemisorption on metal surfaces. (See ref. 179.) $O_2$ on W(100)[243] yielded a value of 0.98 ± 0.03 and $H_2$ on W(100)[244] a value of 0.51 ± 0.03. Data of this precision is certainly important in understanding the incipient energy transfer on adsorption.

Measurement of the angular and velocity distribution of molecules desorbed from solid surfaces utilizes the detection techniques of the molecular beam method regardless of the initial source of the desorbing particles. For example, Van Willigen,[245] and Stickney and coworkers[215,246,247] have used angular and velocity distribution measurements to study the permeation and desorption of $H_2$ from a variety of metal membranes. They found that spatial distributions peaked at the normal and velocity distributions indicative of desorption of particles with excess kinetic energy were observed for carbon and sulfur contaminated Fe, Ni, Nb, Pt and stainless steel surfaces. For clean surfaces the desorbed molecules exhibited cosine distribution. Surprisingly, clean copper surfaces exhibited the same behavior as the contaminated surfaces of the other metals.

(Figure 21.) The copper behavior is attributed to an activation energy barrier for dissociative adsorption of $H_2$ on Cu. Modifications of the molecular beam methods discussed above have been used to measure residence times for surface ionization,[248-250] and the spatial and speed distributions of vaporizing particles.[251,252] All of these techniques and results add to our understanding of energy transfer in the gas-solid interaction.

## E. Ion Scattering

Scattering of ion beams from solid surfaces has been used to study high energy gas-surface interactions. These studies are generally designed to investigate ion implantation,[253-255] irradiation damage, surface sputtering[256-258] and surface composition.[259,262] Energy transfer between incident ions and the solid surface is also conveniently studied using this technique.[258] Since a brief discussion of the experimental technique has been given above, it will suffice to refer the reader to review articles by investigators active in the field[263-265] as well as the original literature cited above. Due to the high energy incident ions usually employed, the information available from these experiments is of a complementary nature to that provided by neutral beam scattering at thermal energies. The analytical uses of the technique are of interest to the surface chemist, while structural information and surface charge state distributions are of value in all areas of surface science.

## 5. Conclusion

The use of molecular beam techniques to study the nature of energy exchange in the gas-solid interaction is increasing rapidly. The purpose of this article has been to give an introduction to the technique to those unfamiliar with this field of surface science, and to provide a collection of data for workers in the field interested in the literature of the last ten years. The authors have not attempted to be exhaustive in collecting all the pertinent literature, but to call attention, in their opinions, to the major experimental and theoretical developments in the field.

As has been mentioned from time to time throughout the body of this article, much work remains to be done in order to more fully understand the mechanism of energy transfer between the gas and the solid surface. In particular, a useable theory of inelastic scattering is necessary for accurate determination of gas-surface interaction potential parameters. This work will certainly be accelerated by the availability of detailed experimental scattering data from a variety of well-characterized solid surfaces. Accurate velocity distribution measurements of particles scattered from well-characterized surfaces will tell a great deal about the energy transfer process if the experimental difficulties can be overcome. The dependence of energy transfer on the internal state of the incident gas molecule is a field where very little work has been done. The use of state selected sources and development of experimental methods to determine the internal state of the scattered beam should shed some light on this important question.

In the field of reactive gas surface interactions, a large variety of systems remain to be investigated. As the understanding of simple reaction systems becomes more clear, these methods will be applied to more complex heterogeneous catalytic reactions. The use of these techniques will hopefully be applied to more and more "realistically" interesting surfaces (such as stepped crystal surfaces), in order to increase our understanding of such important processes as catalysis and corrosion. Of course, developments in the very complex theory of reactive scattering will be welcomed, and the importance of the internal state distribution of reactants and products on this theory should not be ignored.

The problem of energy transfer in the gas-solid interaction is one particularly amenable to study by molecular beam methods. As evidenced by the work cited here and by speculations about future developments, it is a field which will attract the interest of surface scientists of all persuasions. It promises to shed light on important problems in heterogeneous catalysis, oxidation, aerospace sciences, and other branches of surface science.

Acknowledgement

This work was carried out under the auspices of the U. S. Atomic Energy Commission.

## REFERENCES


1. N. F. Ramsey, Molecular Beams, Oxford University Press, London and New York (1956).
2. F. C. Hurlbut, U.C. Engineering Project Report HE-950-208, University of California (1962).
3. R. E. Stickney, Advances in Atomic and Molecular Physics 3, 143 (1967).
4. R. P. Merrill, Catalysis Reviews 4, 115 (1970).
5. J. N. Smith, Jr., Surf. Sci. 34, 613 (1973).
6. M. Knudsen, Ann. Physik 6, 129 (1930).
7. H. H. Rowley and K. F. Bonhoeffer, Z. Phys. Chem. 21, 84 (1933).
8. H. von Ubisch, Arkiv Fysik 10, 157 (1956).
9. L. B. Thomas and E. B. Schofield, J. Chem. Phys. 23, 861 (1955).
10. F. O. Goodman, J. Phys. Chem. Solids 23, 1269 (1962).
11. F. O. Goodman, J. Phys. Chem. Solids 24, 1451 (1963).
12. F. O. Goodman, J. Phys. Chem. Solids 26, 85 (1965).
13. B. McCarroll, J. Chem. Phys. 39, 1317 (1963).
14. H. Shin, J. Chem. Phys. 42, 3442 (1965).
15. R. T. Allen and P. Feuer, J. Chem. Phys. 43, 4500 (1965).
16. S. L. Bernasek and G. A. Somorjai, accepted for publication in J. Chem. Phys. (1974).
17. P. Feuer, J. Chem. Phys. 39, 1311 (1963).
18. E. T. Kinzer and C. M. Chambers, Surf. Sci. 3, 261 (1965).
19. C. M. Chambers and E. T. Kinzer, Surf. Sci. 4, 33 (1966).
20. G. Armand, Surf. Sci. 9, 145 (1968).
21. R. M. Logan, Surf. Sci. 15, 387 (1969).
22. F. O. Goodman and H. Y. Wachman, J. Chem. Phys. 46, 2376 (1967).
23. F. O. Goodman, Surf. Sci. 11, 283 (1968).

24. F. O. Goodman, J. Chem. Phys. 50, 3855 (1969).

25. J. R. Manson, J. Chem. Phys. 56, 3451 (1972).

26. F. O. Goodman and J. D. Gillerlain, J. Chem. Phys. 54, 3077 (1971).

27. F. O. Goodman and J. D. Gillerlain, J. Chem. Phys. 57, 3645 (1972).

28. F. O. Goodman, J. Chem. Phys. 56, 6082 (1972).

29. O. Stern, Naturwiss. 17, 391 (1929).

30. I. Estermann and O. Stern, Z. Physik 61, 95 (1930).

31. J. E. Lennard-Jones and C. Strachan, Proc. Roy. Soc. (London) A 150, 442 (1935).

32. J. E. Lennard-Jones and A. F. Devonshire, Nature 137, 1069 (1936).

33. J. E. Lennard-Jones and A. F. Devonshire, Proc. Roy. Soc. (London) A 156, 6 (1936).

34. N. Cabrera, V. Celli, F. O. Goodman and R. Manson, Surf. Sci. 19, 67 (1970).

35. F. O. Goodman, Surf. Sci. 24, 667 (1971).

36. R. M. Logan and R. E. Stickney, J. Chem. Phys. 44, 195 (1966).

37. R. M. Logan and J. C. Keck, J. Chem. Phys. 49, 860 (1968).

38. R. E. Forman, J. Chem. Phys. 55, 2839 (1971).

39. J. D. Doll, J. Chem. Phys. 59, 1038 (1973).

40. R. M. Logan, J. C. Keck, and R. E. Stickney in Proc. Intern. Symp. Rarified Gas Dyn. 5th Oxford, 1966, 1, 49 (1966).

41. R. E. Stickney in The Structure and Chemistry of Solid Surfaces, (G. A. Somorjai ed., 41-1, 1969).

42. R. E. Stickney, R. M. Logan, S. Yamamoto and J. C. Keck in Fundamentals of Gas Surface Interactions (H. Saltsburg et al., eds.; Academic Press, New York, 1967), 422.

43. F. O. Goodman, J. Chem. Phys. 53, 2281 (1970).

44. K. Karamcheti and L. B. Scott, J. Chem. Phys. 50, 2364 (1969).

45. L. M. Raff, J. Lorenzen, and B. C. McCoy, J. Chem. Phys. 46, 4265 (1967).

46. J. Lorenzen and L. M. Raff, J. Chem. Phys. 49, 1165 (1968).

47. J. Lorenzen and L. M. Raff, J. Chem. Phys. 52, 1133 (1970).

48. J. Lorenzen and L. M. Raff, J. Chem. Phys. 52, 6134 (1970).

49. J. Lorenzen and L. M. Raff, J. Chem. Phys. 54, 674 (1970).

50. J. D. McClure, J. Chem. Phys. 51, 1687 (1969).

51. J. D. McClure, J. Chem. Phys. 52, 2712 (1970).

52. J. D. McClure, J. Chem. Phys. 57, 2810 (1972).

53. J. D. McClure, J. Chem. Phys. 57, 2823 (1972).

54. R. A. Oman, J. Chem. Phys. 48, 3919 (1968).

55. R. A. Oman and V. S. Calia, Grumman Research Dept. Report RE-365, June 1969.

56. R. A. Oman, in Rarified Gas Dynamics, Supp. 4, Vol I, C. L. Brundin ed., Academic Press, New York, 83 (1967).

57. R. A. Oman, A. Bogan, and C. H. Li, in Rarified Gas Dynamics, Supp. 3, Vol II, J. H. de Leeuw ed., Academic Press, New York, 396 (1966).

58. R. A. Oman, V. S. Calia and C. H. Weiser, Grumman Research Dept. Report RE-310, December 1967.

59. V. S. Calia and R. A. Oman, Grumman Research Dept. Report RE-371, September 1969.

60. F. O. Goodman, Surf. Sci. 7, 391 (1967).

61. N. Cabrera and F. O. Goodman, J. Chem. Phys. 56, 4899 (1972).

62. F. O. Goodman, W. S. Liu, and N. Cabrera, J. Chem. Phys. 57, 2698 (1972).

63. M. R. Busby, J. D. Haygood and C. H. Link, Jr., J. Chem. Phys. 54, 4642 (1971).

64. G. Wolken, Jr., J. Chem. Phys. 59, 1159 (1973).

65. K. C. Chang and E. L. Knuth, J. Chem. Phys. 53, 2133 (1970).

66. W. A. Steele, Surf. Sci. 36, 317 (1973).

67. W. A. Steele, Surf. Sci. 38, 1 (1973).

68. R. J. LaBrecque and R. I. Morse, J. Chem. Phys. 56, 546 (1972).

69. J. D. Doll, to be published in J. Chem. Phys., Jan. 15, 1974.

70. E. C. Beder in Adv. Atomic and Molec. Phys. 3, 205 (1967).

71. F. O. Goodman, Surf. Sci. 26, 327 (1971).

72. E. C. Beder, Surf. Sci. 1, 242 (1964).

73. A. J. Howsmon, in Proc. Intern. Symp. Rarified Gas Dyn., 4th Toronto, 2, 417 (1966), and 5th Oxford, 1, 67 (1967).

74. A. Tsuchida, Surf. Sci. 14, 375 (1969).

75. F. O. Goodman, Surf. Sci. 19, 93 (1970).

76. R. Manson and V. Celli, Surf. Sci. 24, 495 (1971).

77. F. O. Goodman, J. Chem. Phys. 55, 5742 (1971).

78. F. O. Goodman, Surf. Sci. 27, 157 (1971).

79. J. L. Beeby, J. Phys. C: Solid State Physics 4, L359 (1971).

80. J. L. Beeby, J. Phys. C: Solid State Physics 5, 3438 (1972).

81. J. L. Beeby, J. Phys. C: Solid State Physics 5, 3457 (1972).

82. W. H. Weinberg, J. Phys. C: Solid State Physics 5, 2098 (1972).

83. F. O. Goodman, Surf. Sci. 30, 1 (1972).

84. G. A. Somorjai, Principles of Surface Chemistry, Prentice-Hall, Inc., Englewood Cliffs, New Jersey (1972).

85. F. O. Goodman and W. K. Tan, J. Chem. Phys. 59, 1805 (1973).

86. F. O. Goodman, J. Chem. Phys. 58, 5530 (1973).

87. F. O. Goodman and W. K. Tan, J. Chem. Phys. 58, 5527 (1973).

88. P. O. Schissel and O. C. Trulson, J. Chem. Phys. 43, 737 (1965).

89. L. A. West and G. A. Somorjai, J. Vac. Sci. Technol. 9, 668 (1972). W. H. Weinberg, J. Catal. 28, 459 (1973).

90. R. J. Madix and A. Susu, J. Catal. 28, 316 (1973).

91. D. R. Olander, W. J. Siekhaus, R. Jones and J. A. Schwarz, J. Chem. Phys. 57, 408 (1972).

92. H. Wise and B. J. Wood in Adv. in Atomic and Molec. Phys. 3, 291 (1967).

93. W. H. Weinberg and R. P. Merrill, Suf. Sci. 33, 493 (1972).

94. W. H. Weinberg, R. M. Lambert, C. M. Comrie and J. W. Linnett, Surf. Sci. 30, 299 (1972).

95. W. H. Weinberg, J. Vac. Sci. Technol. 10, 89 (1973).

96. P. J. Pagni and J. C. Keck, J. Chem. Phys. 58, 1162 (1973).

97. H. Deuss and A. van der Avoird, Phys. Rev. B 8, 2441 (1973).

98. M. Remy, J. Chem. Phys. 53, 2487 (1970).

99. N. D. Lang and W. Kohn, Phys. Rev. B 7, 3541 (1973).

100. R. C. Logani and W. W. Smeltzer, Can. Metall. Quart. 10, 149 (1971) and references therein.

101. R. C. Baetzold, J. Cat. 29, 129 (1973).

102. O. Johnson, J. Cat. 28, 503 (1973).

103. R. W. Maatman, Cat. Rev. 8, 1 (1973).

104. R. P. Messmer and A. J. Bennett, Phys. Rev. B 6, 633 (1972).

105. G. C. Bond, Catalysis by Metals, Academic Press, New York, 1962, p. 128, 240.

106. Ibid., p. 128, 225.

107. J. C. Batty and R. E. Stickney, J. Chem. Phys. 51, 4475 (1969).

108. B. Weber and A. Cassuto, Surf. Sci. 39, 83 (1973).

109. G. E. Busch, J. F. Cornelius, R. T. Mahoney, R. L. Morse, D. W. Schlosser, and R. K. Wilson, Rev. Sci. Instrum. 41, 1066 (1970).

110. S. Dushman, Scientific Foundations of Vacuum Technique, 2nd ed., John Wiley and Sons, Inc., New York (1962).

111. L. A. West, Ph.D. dissertation, University of California, Berkeley (1971).

112. L. A. West, E. I. Kozak and G. A. Somorjai, J. Vac. Sci. Technol. 8, 430 (1971).

113. R. A. Krakowski and D. R. Olander, J. Chem. Phys. 49, 5027 (1968).

114. J. N. Smith, Jr., and H. Saltsburg, J. Chem. Phys. 40, 3585 (1964).

115. D. L. Smith and R. P. Merrill in Proc Intern. Symp. Rarified Gas Dyn., 6th M.I.T., 1968, 2, 1159 (1969).

116. G. A. Somorjai and H. H. Farrell in Advances Chem. Phys. 20, 215 (1971). I. Prigogine and S. A. Rice eds., John Wiley and Sons, Inc., New York 1971.

117. C. C. Chang, Surf. Sci. 25, 53 (1971).

118. W. A. Fraser, J. V. Florio, W. N. Delgass and W. D. Robertson, Rev. Sci. Instrum. 44, 1490 (1973).

119. T. L. Bradley, A. E. Dabiri and R. E. Stickney, Surf. Sci. 29, 590 (1972).

120. W. J. Moore, Physical Chemistry, Prentice-Hall, Inc., Englewood Cliffs, New Jersey, 3rd ed. (1962).

121. R. H. Jones, D. R. Olander and V. R. Kruger, J. App. Phys. 40, 4641 (1969).

122. D. R. Olander, J. App. Phys. 40, 4650 (1969).

123. D. R. Olander and V. Kruger, J. App. Phys. 41, 2769 (1970).

124. D. R. Olander, R. H. Jones and W. J. Siekhaus, J. App. Phys. 41, 4388 (1970).

125. W. J. Siekhaus, R. H. Jones and D. R. Olander, J. App. Phys. 41, 4392 (1970).

126. D. R. Olander and R. H. Jones, Entropie 30, 42 (1969).

127. R. H. Jones, V. R. Kruger and D. R. Olander, Lawrence Radiation Laboratory Report UCRL-17859, University of California, Berkeley (1968).

128. S. L. Bernasek and G. A. Somorjai, Lawrence Berkeley Laboratory Report LBL-1140, University of California, Berkeley (1972).

129. J. B. Anderson, R. P. Andres and J. B. Fenn, Adv. Chem. Phys. 10, 275 (1966).

130. A. Kantrowitz and J. Grey, Rev. Sci. Instr. 22, 328 (1951).

131. G. B. Kistiakowsky and W. P. Schlichter, Rev. Sci. Instr. 22, 333 (1951).

132. J. B. Anderson, R. P. Andres and J. B. Fenn, Adv. At. Molec. Physics 1, 345 (1965).

133. E. L. Knuth, App. Mech. Reviews 17, 751 (1964).

134. H. V. Hostettler and R. B. Bernstein, Rev. Sci. Instr. 31, 872 (1960).

135. R. G. J. Fraser, Molecular Rays, Cambridge Univ. Press, London (1931).

136. See other articles contained in refs. 129 and 132, for example.

137. K. Kodera, I. Kusunoki, K. Horinouchi, K. Isa and M. Yoshihara, Japan. J. App. Phys. 10, 543 (1971).

138. J. N. Smith, Jr., and W. L. Fite in Rarified Gas Dynamics, Supp. 2, Vol. I, J. A. Laurman, ed. (Academic Press, New York 1963).

139. R. A. Krakowski, Ph.D. dissertation, University of California, Berkeley (1967).

140. F. M. Devienne, B. Crave, J. Souquet and R. Chapier in Rarified Gas Dynamics, Supp. 2, Vol. I, J. A. Laurman ed., Academic Press, New York (1963).

141. S. Yamamoto and R. E. Stickney, J. Chem. Phys. 47, 1091 (1967).

142. I. L. Kofsky and H. Levinstein, Phys. Rev. 74, 500 (1948).

143. E. W. Becker and W. Henkes, Z. Physik 146, 320 (1956).

144. O. F. Hagena and A. K. Varma, Rev. Sci. Instr. 39, 47 (1968).

145. K. Jakus and F. C. Hurlbut in The Structure and Chemistry of Solid Surfaces, G. A. Somorjai ed., John Wiley and Sons, Inc., New York, 44-1 (1968).

146. A. E. Dabiri, T. J. Lee, and R. E. Stickney, Surf. Sci. 26, 522 (1971).

147. H. Harrison, D. G. Hummer, and W. L. Fite, J. Chem. Phys. 41, 2567 (1964).

148. W. J. Siekhaus, J. A. Schwarz and D. R. Olander, Surf. Sci. 33, 445 (1972).

149. R. H. Jones, D. R. Olander, W. J. Siekhaus and J. A. Schwarz, J. Vac. Sci. Tech. 9, 1429 (1972).

150. M. R. Zatrick, Electro-Optical Sys. Des. June 1972 p. 20.

151. M. R. Zatrick, Research/Development 21, 16 (1970).

152. F. W. Karasek, Research/Development 22, 51 (1971).

153. J. A. Schwarz and R. J. Madix, J. Catal. 12, 140 (1968).

154. R. H. Jones, Ph.D. dissertation, University of California, Berkeley (1971).

155. D. R. Olander, in The Structure and Chemistry of Solid Surfaces, G. A. Somorjai ed., John Wiley and Sons, Inc., New York, 45-1 (1968).

156. M. Kaminsky, Advanced Energy Conversion 3, 255 (1963).

157. C. A. Visser, J. Wolleswinkel and J. Los, J. Phys. E: Scient. Inst. 3, 483 (1970).

158. I. Estermann, R. Frisch, and O. Stern, Z. Physik 73, 348 (1931).

159. J. C. Crews, J. Chem. Phys. 37, 2004 (1962).

160. D. R. O'Keefe, R. L. Palmer, H. Saltsburg and J. N. Smith, Jr., J. Chem. Phys. 49, 5194 (1968).

161. J. N. Smith, Jr., D. R. O'Keefe and R. L. Palmer, J. Chem. Phys. 52, 315 (1970).

162. D. R. O'Keefe, J. N. Smith, Jr., R. L. Palmer, and H. Saltsburg, Surf. Sci. 20, 27 (1970).

163. D. R. O'Keefe, J. N. Smith, Jr., R. L. Palmer and H. Saltsburg, J. Chem. Phys. 52, 4447 (1970).

164. B. R. Williams, J. Chem. Phys. 55, 1315 (1971).

165. B. R. Williams, J. Chem. Phys. 55, 3220 (1971).

166. H. Hoinkes, H. Nahr and H. Wilsch, Surf. Sci. 30, 363 (1972).

167. D. E. Houston and D. R. Frankl, Phys. Rev. Lett. 31, 298 (1973).

168. D. V. Tendulkar and R. E. Stickney, Surf. Sci. 27, 516 (1971).

169. W. H. Weinberg and R. P. Merrill, Phys. Rev. Lett. 25, 1198 (1970).

170. W. H. Weinberg and R. P. Merrill, J. Chem. Phys. 56, 2893 (1972).

171. R. Chappell and D. O. Hayward, J. Vac. Sci. Tech. 9, 1052 (1972).

172. R. Chappell and D. O. Hayward, Imperial College preprint, London (1971).

173. B. F. Mason and B. R. Williams, J. Chem. Phys. 56, 1895 (1972).

174. H. Hoinkes, H. Nahr, and H. Wilsch, Surf. Sci. 33, 516 (1972).

175. H. Saltsburg and J. N. Smith, Jr., J. Chem. Phys. 45, 2175 (1966).

176. J. N. Smith, Jr., H. Saltsburg, and R. L. Palmer, J. Chem. Phys. 49, 1287 (1968).

177. R. L. Palmer, H. Saltsburg and J. N. Smith, Jr., J. Chem. Phys. 50, 4661 (1969).

178. R. Sau and R. P. Merrill, Surf. Sci. 34, 268 (1973).

179. S. L. Bernasek, W. J. Siekhaus and G. A. Somorjai, Phys. Rev. Lett. 30, 1202 (1973).

180. R. B. Subbarao and D. R. Miller, J. Chem. Phys. 51, 4679 (1969).

181. M. J. Romney and J. B. Anderson, J. Chem. Phys. 51, 2490 (1969).

182. D. R. Miller and R. B. Subbarao, J. Chem. Phys. 52, 425 (1970).

183. V. S. Calia and R. A. Oman, J. Chem. Phys. 52, 6184 (1970).

184. W. J. Hays, W. E. Rodgers, and E. L. Knuth, J. Chem. Phys. 56, 1652 (1972).

185. R. A. Oman, A. Bogan, C. Weiser, and C. H. Li , AIAAJ. 2, 10 (1964).

186. M. N. Bishara and S. S. Fisher, J. Chem. Phys. 52, 5661 (1970).

187. J. Lapujoulade, Y. Lejay and G. Armand, preprint, Saclay (1972).

188. R. B. Subbarao and D. R. Miller, J. Chem. Phys. 58, 5247 (1973).

189. D. L. Smith and R. P. Merrill, J. Chem. Phys. 53, 3588 (1970).

190. W. H. Weinberg and R. P. Merrill, J. Chem. Phys. 56, 2881 (1972).

191. L. A. West and G. A. Somorjai, J. Chem. Phys. 54, 2864 (1971).

192. L. A. West and G. A. Somorjai, J. Chem. Phys. 57, 5143 (1972).

193. D. L. Smith and R. P. Merrill, in proc. California Catalysis Society meeting, Santa Barbara, October 1968.

194. R. P. Merrill and D. L. Smith, Surf. Sci. 21, 203 (1970).

195. A. G. Stoll, D. L. Smith and R. P. Merrill, J. Chem. Phys. 54, 163 (1971).

196. A. R. Rudnicki, Jr., and H. Y. Wachman, Surf. Sci. 34, 679 (1973).

197. W. C. Steele, Avco Corporation Technical Report AVSD-0509-70-CR, September 1970.

198. W. J. Siekhaus, J. A. Schwarz and D. R. Olander, Surf. Sci. 33, 445 (1972).

199. G. Daury, A. Constans, P. Lostis, and D. A. Degras, Surf. Sci. 14, 103 (1969).

200. J. N. Smith, Jr., J. Chem. Phys. 40, 2520 (1964).

201. S. S. Fisher, O. F. Hagena, and R. G. Wilmoth, J. Chem. Phys. 49, 1562 (1968).

202. H. Saltsburg, J. N. Smith, Jr., and R. L. Palmer, in The Structure and Chemistry of Solid Surfaces, G. A. Somorjai ed., John Wiley and Sons, Inc., New York (1969).

203. R. L. Palmer, J. N. Smith, Jr., H. Saltsburg, and D. R. O'Keefe, J. Chem. Phys. 53, 1666 (1970).

204. S. Yamamoto and R. E. Stickney, J. Chem. Phys. 53, 1594 (1970).

205. M. D. Scheer, R. Klein, and J. D. McKinley, Surf. Sci. 30, 251 (1972).

206. D. F. Ollis, H. G. Lintz, A. Pentenero, and A. Cassuto, Surf. Sci. 26, 21 (1971).

207. H. G. Lintz and A. Pentenero, Surf. Sci. 30, 499 (1972).

208. J. C. Crews, J. Chem. Phys. 37, 2004 (1962).

209. J. N. Smith, D. R. O'Keefe, H. Saltsburg, and R. L. Palmer, J. Chem. Phys. 50, 4667 (1969).

210. D. R. O'Keefe, R. L. Palmer and J. N. Smith, Jr., J. Chem. Phys. 55, 4572 (1971).

211. R. O. Frisch and O. Stern, Zeits. f. Physik 84, 443 (1933).

212. G. C. Bond, Catalysis by Metals, Academic Press, New York (1962).

213. J. Smith and W. Fite, J. Chem. Phys. 37, 898 (1962).

214. R. L. Palmer, J. N. Smith, Jr., H. Saltsburg and D. R. O'Keefe, J. Chem. Phys. 53, 1666 (1970).

215. T. L. Bradley and R. E. Stickney, Surf. Sci. 38, 313 (1973).

216. S. L. Bernasek, W. J. Siekhaus, and G. A. Somorjai, to be published. Presented at symposium on Molecular Beam Scattering, Division of Colloid and Surface Science, ACS meeting, Los Angeles, April 1974.

217. R. N. Coltharp, J. T. Scott and E. E. Muschlitz, Jr., J. Chem. Phys. 51, 5180 (1969).

218. R. N. Coltharp, J. T. Scott and E. E. Mushlitz, Jr., in The Structure and Chemistry of Solid Surfaces, G. A. Somorjai, ed., John Wiley and Sons, Inc., New York, 66-1 (1969).

219. C. W. Nutt and S. Kapur, Nature 220, 697 (1968).

220. A. Z. Ullman, private communication.

221. J. N. Smith, Jr., and R. L. Palmer, J. Chem. Phys. 56, 13 (1972).

222. J. N. Smith, Jr., R. L. Palmer and D. A. Vroom, J. Vac. Sci. Tech. 10, 373 (1973).

223. T. R. Acharya, D. R. Olander and A. Z. Ullman, presented at 33rd Conference on Physical Electronics, Berkeley (1973).

224. J. McCarty, J. Falconer and R. J. Madix, J. Catal. 30, 235 (1973).

225. R. J. Madix, J. Falconer, J. McCarty, J. Catal. 31, 316 (1973).

226. J. D. McKinley, J. Chem. Phys. 40, 120 (1964).

227. J. D. McKinley, J. Chem. Phys. 40, 576 (1964).

228. J. B. Anderson and M. Boudart, J. Catal. 3, 216 (1964).

229. R. J. Madix and M. Boudart, J. Catal. 7, 240 (1967).

230. R. J. Madix and R. Korus, Trans. Far. Soc. 64, 2514 (1968).

231. R. J. Madix and A. A. Susu, Surf. Sci. 20, 377 (1970).

232. R. J. Madix, R. Parks, A. A. Susu, and J. A. Schwarz, Surf. Sci. 24, 288 (1971).

233. R. J. Madix and J. A. Schwarz, Surf. Sci. 24, 264 (1971).

234. D. R. Olander, R. H. Jones, J. A. Schwarz and W. J. Siekhaus, J. Chem. Phys. 57, 421 (1972).

235. W. C. Steele, Technical Report AFML-TR-65-343, part II, Avco Missiles, Space and Electronics Group, Wilmington, Massachusetts (1967).

236. A. Z. Ullman and R. J. Madix, presented at 33rd Conference on Physical Electronics, Berkeley (1973).

237. N. Pacia, H. G. Lintz and A. Pentenero, Surf. Sci. 36, 701 (1973).

238. R. E. Stickney, Phys. of Fluids 5, 1617 (1962).

239. N. Abauf and D. G. H. Marsden, Rarified Gas Dynamics Supp. 4, Vol. I, 199 (1967).

240. R. Klein, Surf. Sci. 11, 227 (1968).

241. J. A. Riley and C. F. Giese, J. Chem. Phys. 53, 146 (1970).

242. D. A. King and M. G. Wells, Surf. Sci. 29, 454 (1972).

243. T. E. Madey, Surf. Sci. 33, 355 (1972).

244. T. E. Madey, Surf. Sci. 36, 281 (1973).

245. W. Van Willigen, Phys. Lett. 28A, 80 (1968).

246. A. E. Dabiri, T. J. Lee and R. E. Stickney, Surf. Sci. 26, 522 (1971).

247. T. L. Bradley, A. E. Dabiri, and R. E. Stickney, Surf. Sci. 29, 590 (1972).

248. J. N. Smith, Jr., J. Wolleswinkel and J. Los, Surf. Sci. 22, 411 (1970).

249. T. J. Lee and R. E. Stickney, Surf. Sci. 32, 100 (1972).

250. R. Müller and H.-W. Wassmuth, Surf. Sci. 34, 249 (1973).

251. M. Balooch, A. E. Dabiri and R. E. Stickney, Surf. Sci. 30, 483 (1972).

252. R. F. Burns, J. Chem. Phys. 52, 2152 (1970).

253. W. J. Siekhaus, Ph.D. dissertation, University of California, Berkeley (1965).

254. D. W. Vance, J. App. Phys. 42, 5430 (1971).

255. L. Eriksson, J. A. Davies, N. G. E. Johansson and J. W. Mayer, J. App. Phys. 40, 842 (1969).

256. P. Dahl and N. Sandager, Surf. Sci. 14, 305 (1969).

257. E. P. Th. M. Suurmeijer, A. L. Boers and S. H. A. Begemann, Surf. Sci. 20, 424 (1970).

258. W. Heiland, H. G. Schäffler and E. Taglauer, Surf. Sci. 35, 381 (1973).

259. O. Meyer, J. Gyulai and J. W. Mayer, Surf. Sci. 22, 263 (1970).

260. D. P. Smith, Surf. Sci. 25, 171 (1971).

261. D. J. Ball, T. M. Buck, D. Macnair and G. H. Wheatley, Surf. Sci. 30, 69 (1972).

262. H. H. Brongersma and P. M. Mul, Surf. Sci. 35, 393 (1973).

263. J. W. Mayer and O. J. Marsh, in Applied Solid State Science, Vol. I, p. 239 (Academic Press, New York, 1969).

264. I. Bergström and B. Domeji, Nucl. Inst. and Methods 43, 146 (1966).

265. R. G. Wilson and G. R. Brewer, Ion Beams, J. Wiley and Sons, Inc., New York (1973).

266. J. D. Doll, to be published, Chem. Phys. 3 in 1974.

## FIGURE CAPTIONS

Figure 1 - Schematic diagram of gas-solid interaction.

Figure 2 - Scattering distribution of $N_2$, $H_2$ and Ar scattered from clean Pt(111) (lower plot) and CO covered Pt(111) (upper plot). Arrow indicates angle of incidence.

Figure 3 - Model for quantum theory of inelastic scattering.

Figure 4 - Hard cube scattering model (ref. 36).

Figure 5 - Comparison of experimental (o) and theoretical (solid line) scattering distributions for Argon from platinum using the hard cube model. (Ref. 41.)

Figure 6 - Soft cube scattering model. (Ref. 37.)

Figure 7 - Modified rigid rotor hard cube scattering model. (Ref. 39.)

Figure 8 - Schematic of UHV molecular beam surface scattering apparatus.

Figure 9 - Comparison of geometry, intensity, pumping requirements, angular and velocity distributions for three molecular beam sources.

Figure 10 - Photomicrograph of multichannel capillary array source.

Figure 11 - Schematic diagram of rotating disk velocity selector. Transmitted velocity u is $u = \frac{nl\omega}{2\pi}$ where l is distance between disks, n is the number of slits and $\omega$ is the angular frequency in radians $sec^{-1}$.

Figure 12 - Comparison of ion gauge and mass spectrometer detectors, showing difference between flux sensitive and density sensitive configurations.

Figure 13 - Schematic diagram of quadrupole mass spectrometer.

Figure 14 - Schematic diagram of lock-in amplifier.

Figure 15 - Schematic diagram of W(112) surface. (Ref. 168.)

Figure 16 - Scattering distributions of hydrogenic molecules from Ni(111). (Ref. 177.)

Figure 17 - Comparison of experimental and theoretical positions of scattering distribution maxima. Incident angle: 50°. Triangles: experimental. Squares: soft cube model. Circles: Oman's calculations. Solid curve: hard cube model. (Ref. 181.)

Figure 18 - Scattering distribution of He from LiF showing phonon loss peaks. (Refs. 164,165.)

Figure 19 - Scattering distribution of $H_2$, $D_2$ and HD formed at the surface from Pt(111) and Pt(997) single crystal surfaces. Drawing above distribution is schematic of surface structure. (Ref. 179.)

Figure 20 - Angular desorption distributions for $H_2$ diffusion through contaminated Fe, Pt, Nb and stainless steel surfaces (left) and clean and contaminated Cu surfaces (right). (Ref. 215.)

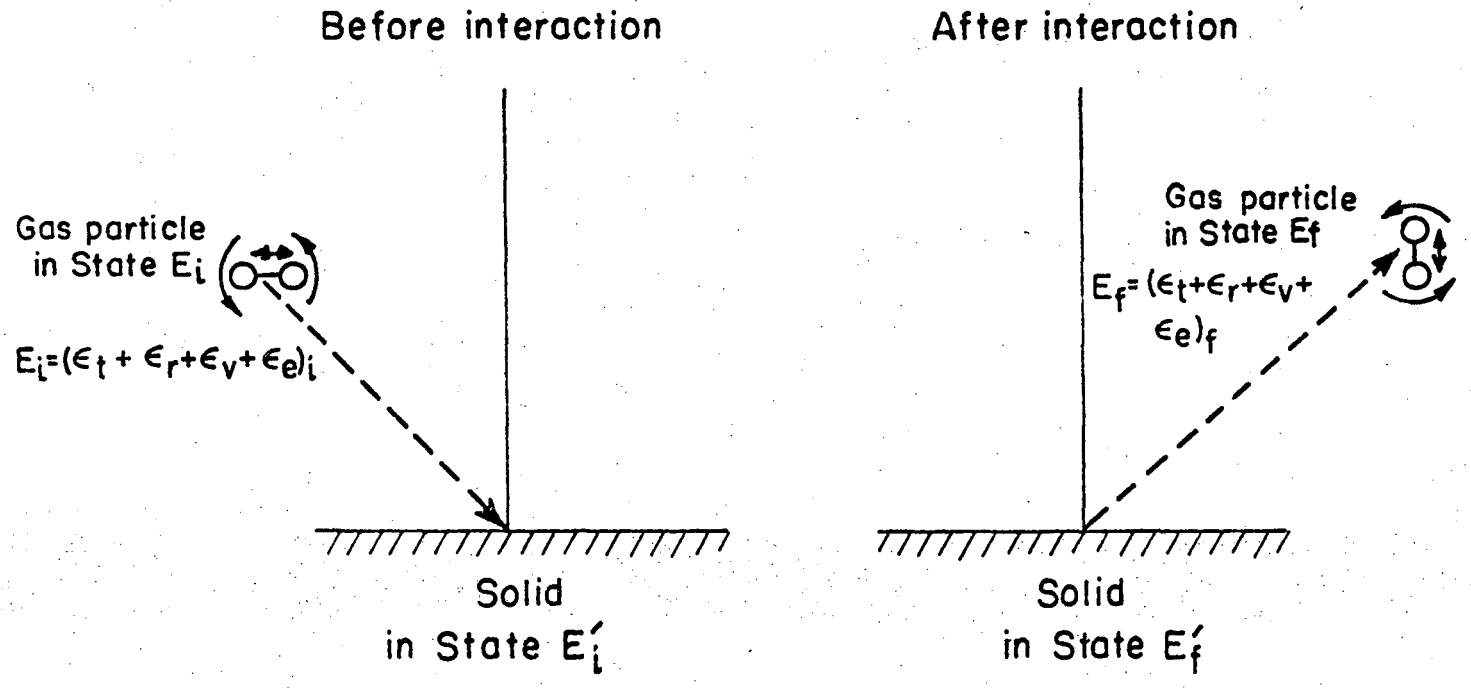
Before interaction
After interaction
Gas particle
in State $E_i$
$E_i=(\epsilon_t+\epsilon_r+\epsilon_v+\epsilon_e)_i$
Solid
in State $E_i'$
Gas particle
in State $E_f$
$E_f=(\epsilon_t+\epsilon_r+\epsilon_v+\epsilon_e)_f$
Solid
in State $E_f'$
XBL741-5526

Fig. 1

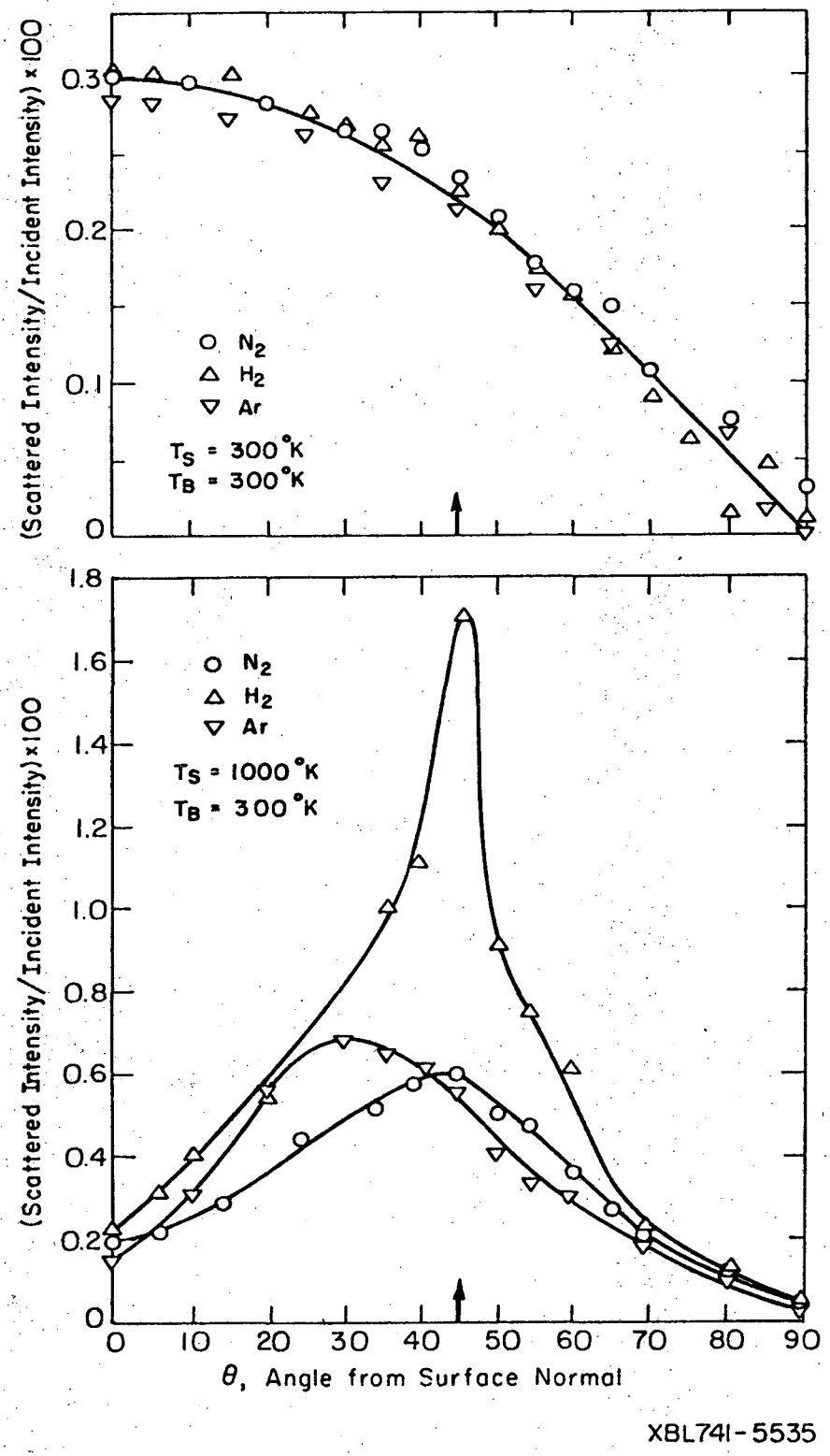
(Scattered Intensity/Incident Intensity) x 100
0.3
0.2
0.1
0
O N2
Δ H2
▽ Ar
TS = 300°K
TB = 300°K
1.8
1.6
1.4
1.2
1.0
0.8
0.6
0.4
0.2
0
O N2
Δ H2
▽ Ar
TS = 1000°K
TB = 300°K
0 10 20 30 40 50 60 70 80 90
θ, Angle from Surface Normal
XBL741-5535

Fig. 2

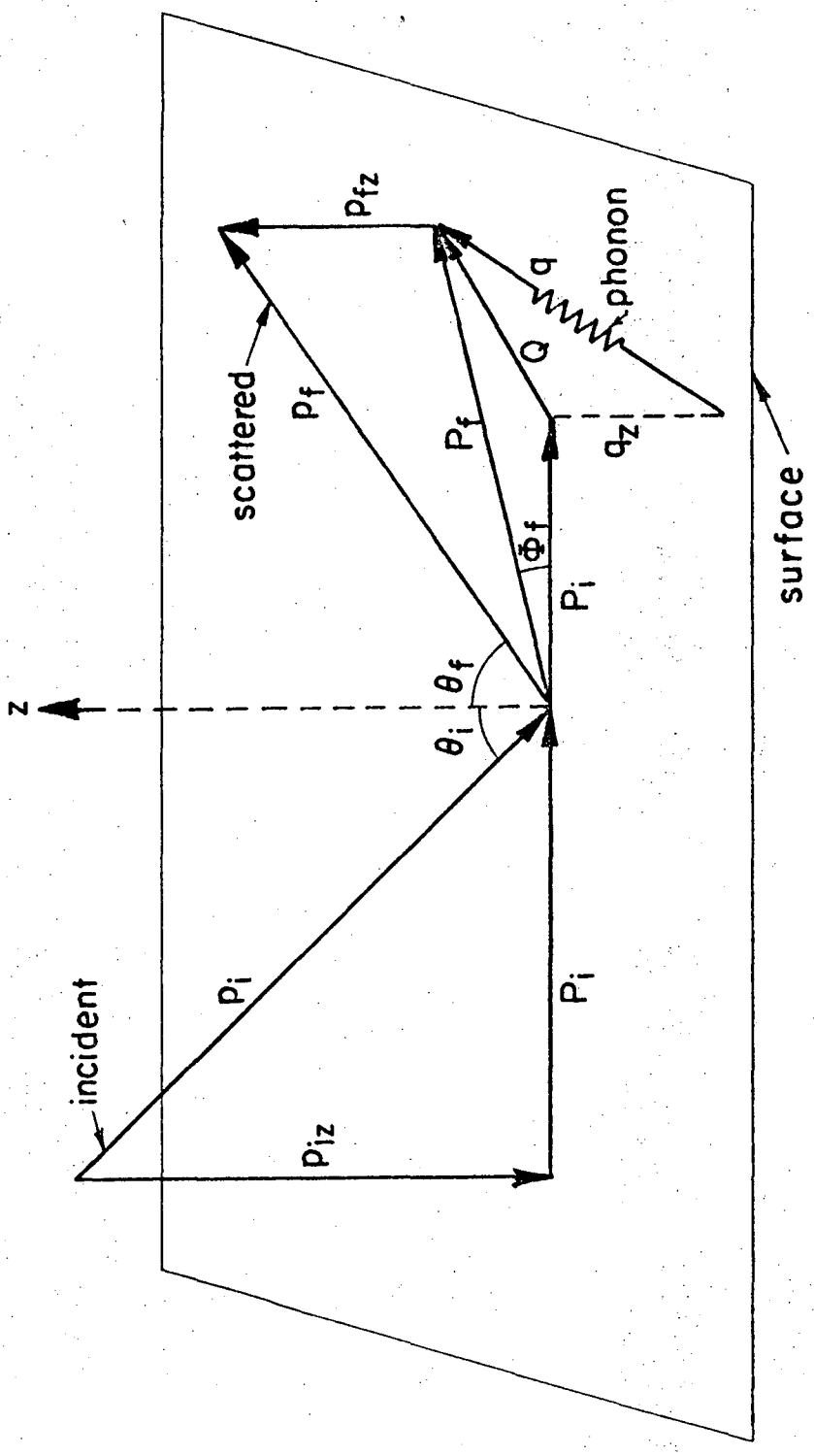


XBL741-5527

Fig. 3

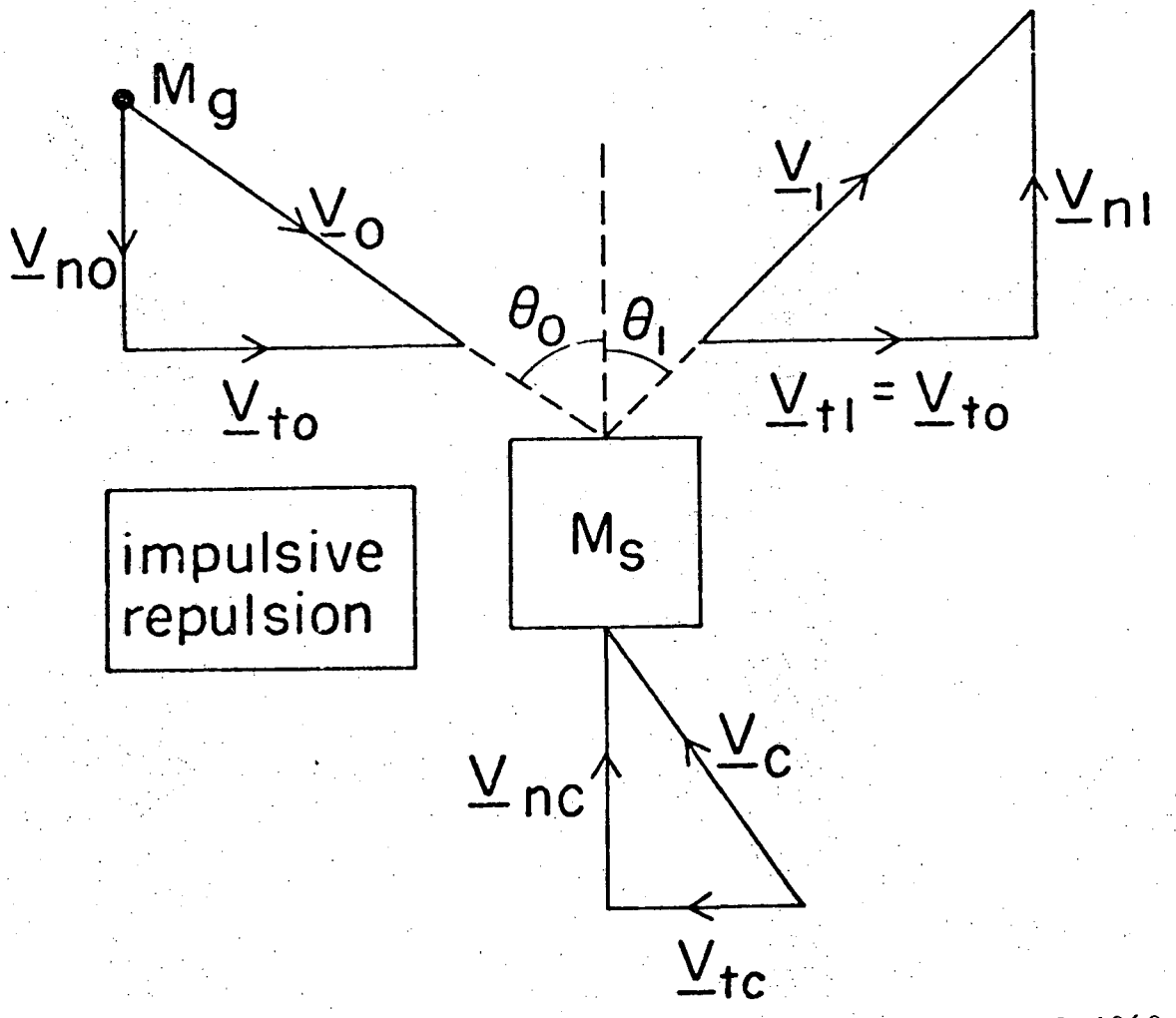


XBL 738-1060

Fig. 4

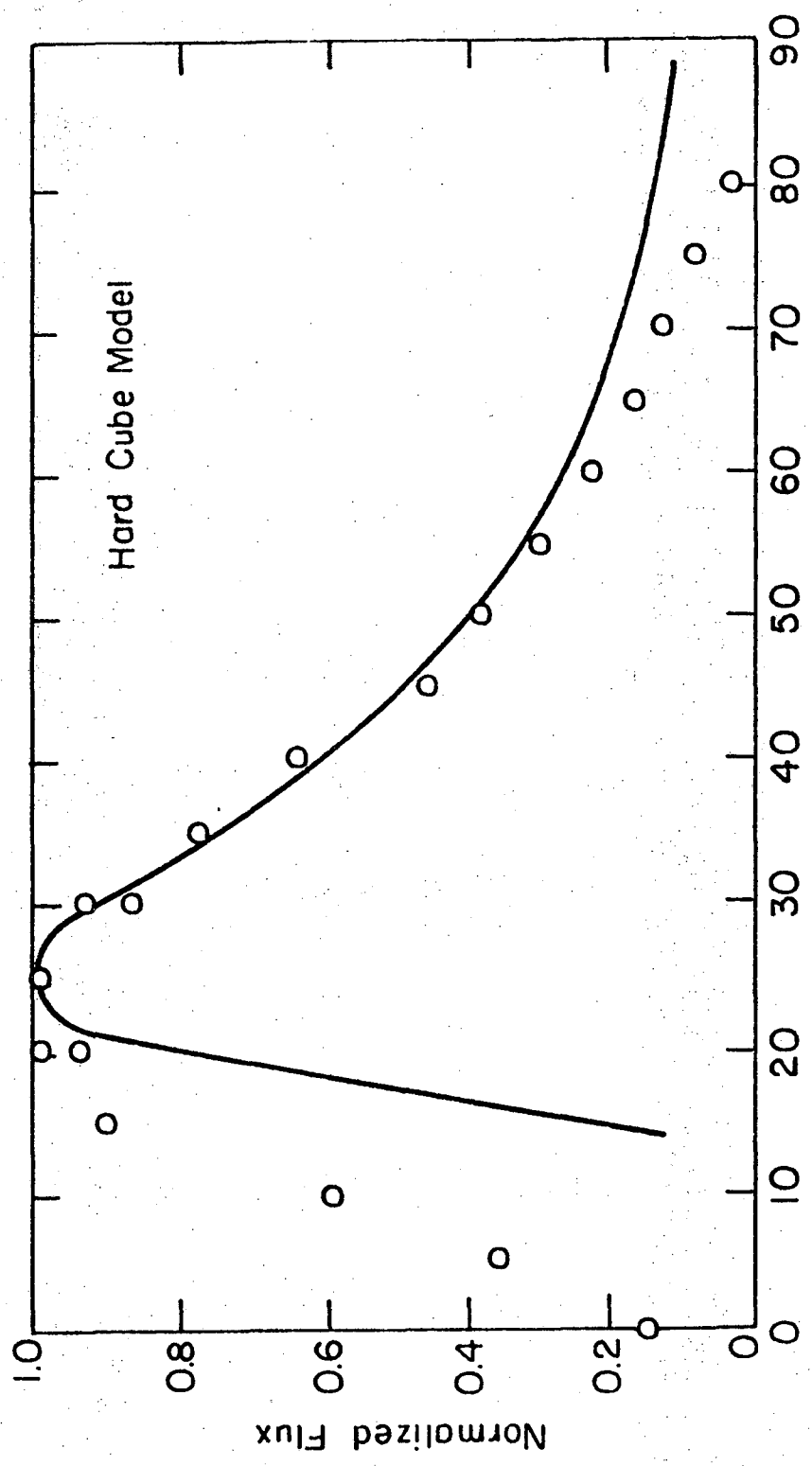
Hard Cube Model
Normalized Flux
1.0
0.8
0.6
0.4
0.2
0
0
10
20
30
40
50
60
70
80
90
$\theta_r$, degrees
XBL741-5528

Fig. 5

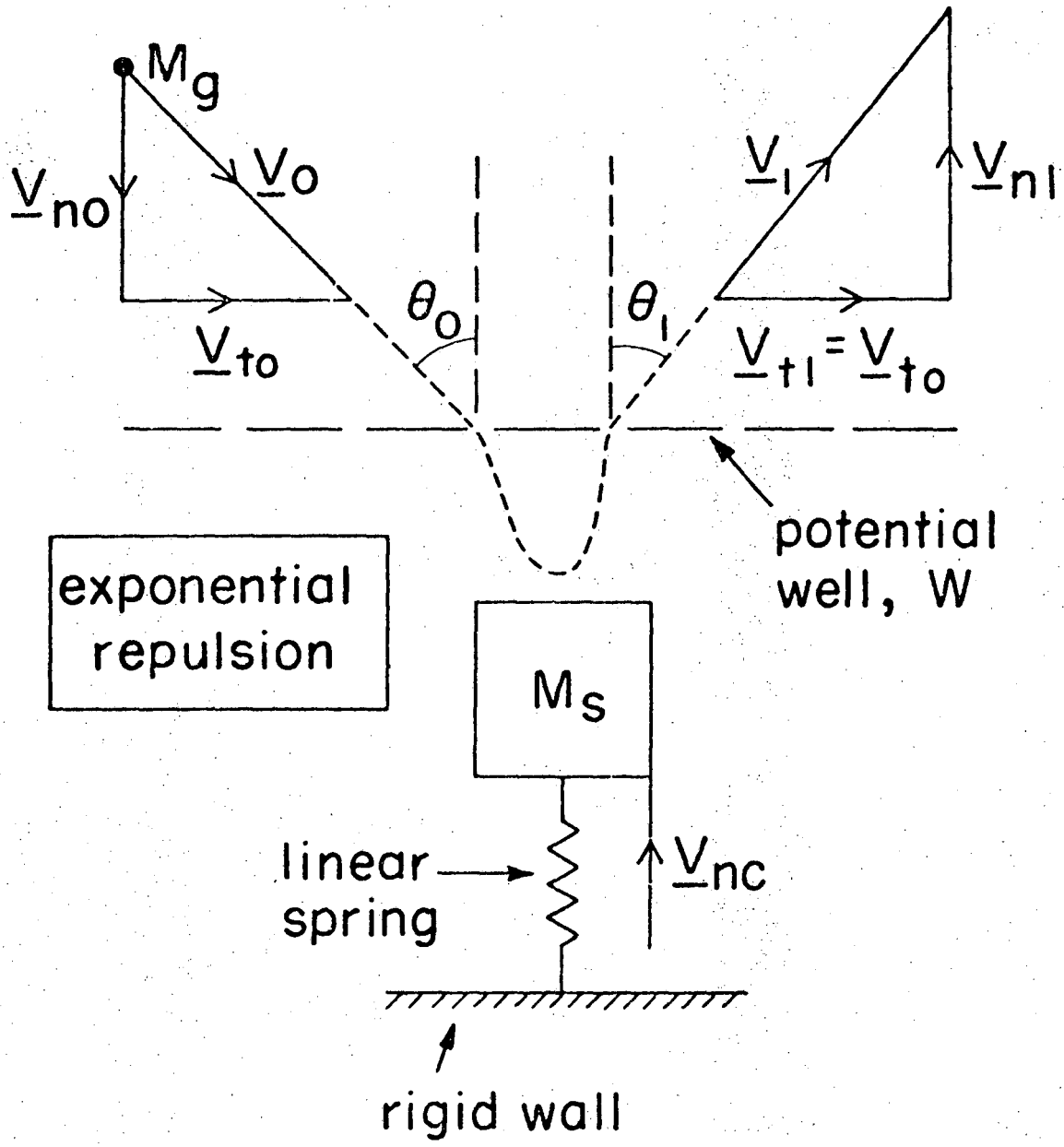


XBL 738-1062

Fig. 6

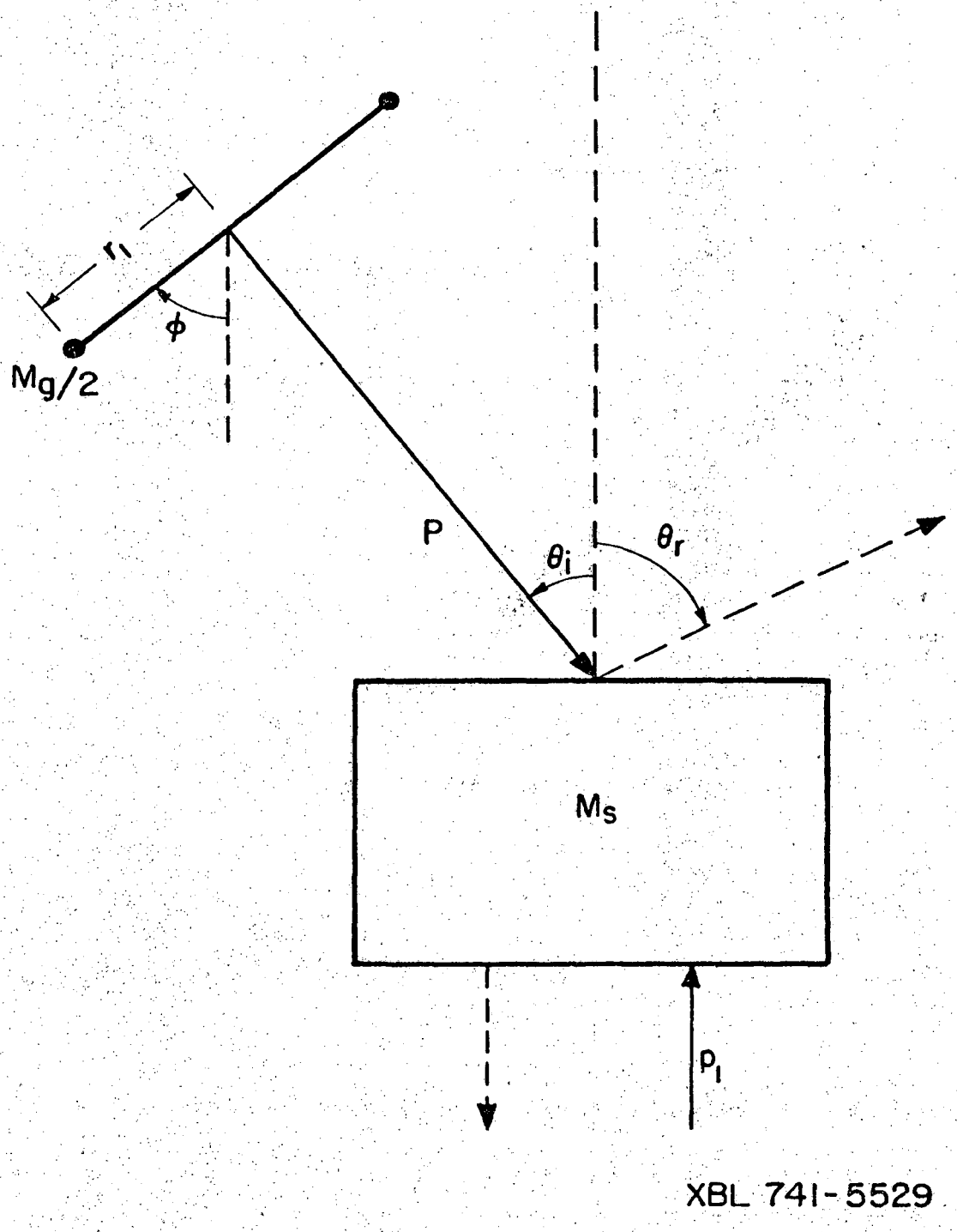


Fig. 7

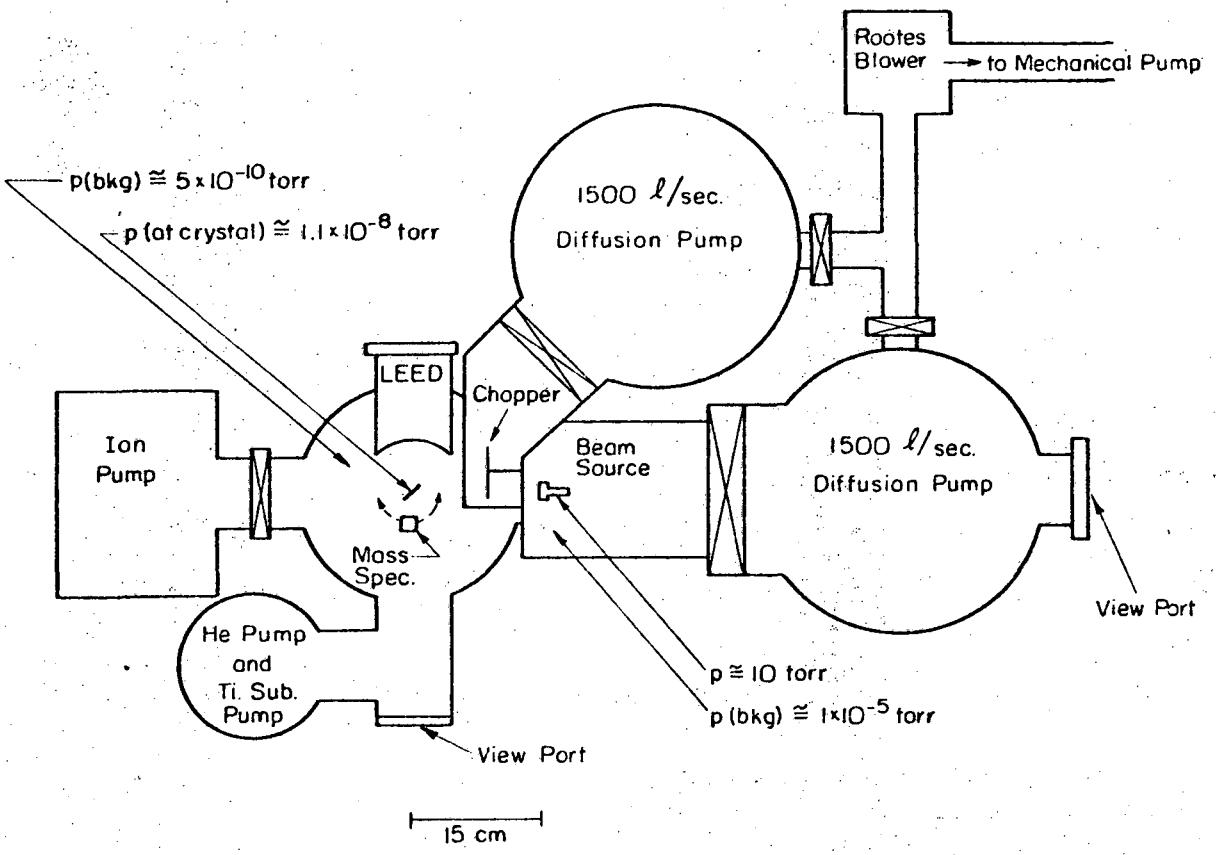


MOLECULAR BEAM SURFACE SCATTERING APPARATUS

XBL 732-5744

Fig. 8

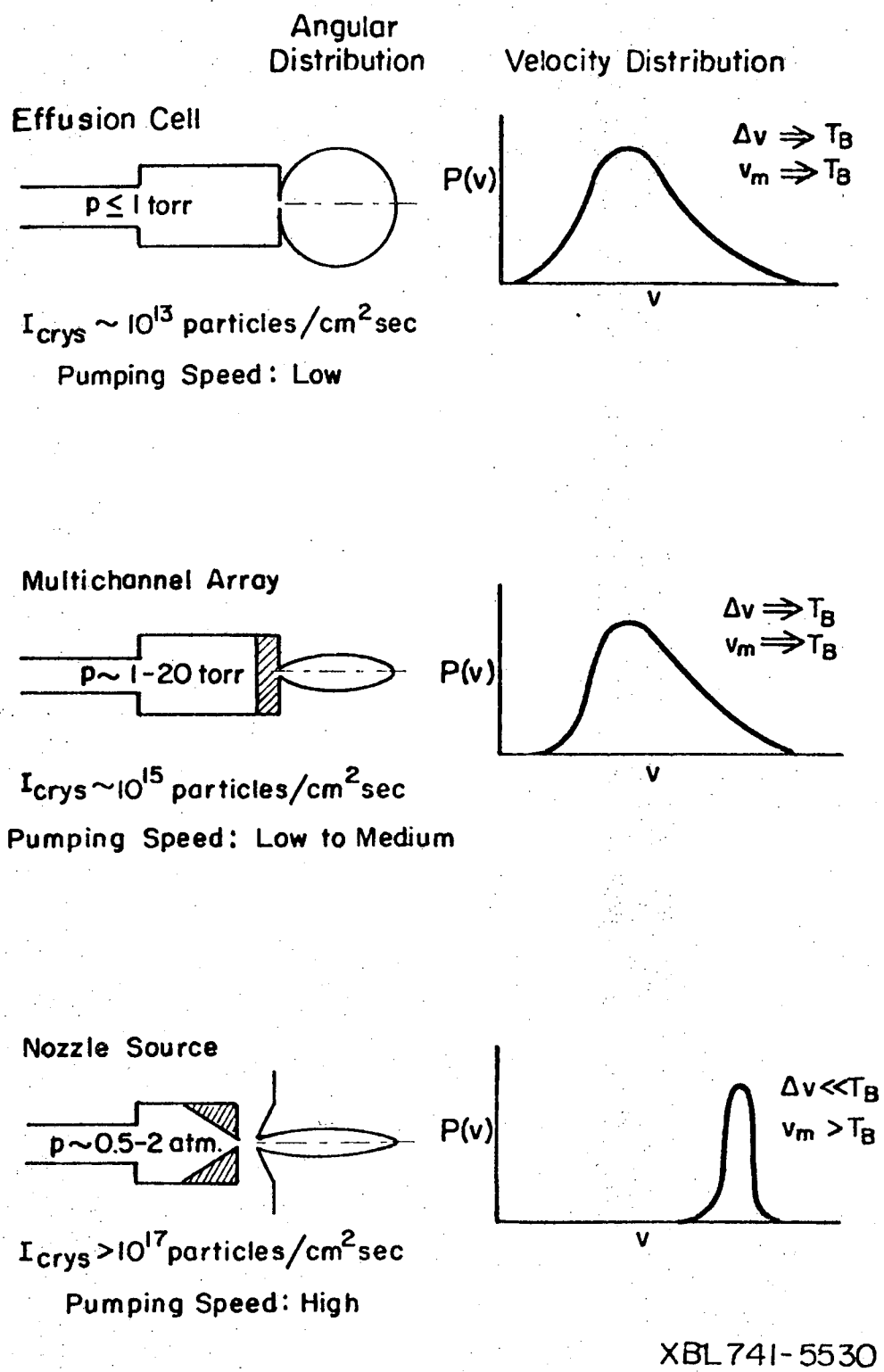
Angular Distribution
Velocity Distribution
Effusion Cell
p ≤ 1 torr
P(v)
v
Δv ⇒ T_B
v_m ⇒ T_B
I_crys ~ 10^13 particles/cm^2 sec
Pumping Speed: Low
Multichannel Array
p ~ 1-20 torr
P(v)
v
Δv ⇒ T_B
v_m ⇒ T_B
I_crys ~ 10^15 particles/cm^2 sec
Pumping Speed: Low to Medium
Nozzle Source
p ~ 0.5-2 atm.
P(v)
v
Δv << T_B
v_m > T_B
I_crys > 10^17 particles/cm^2 sec
Pumping Speed: High
XBL741-5530

Fig. 9

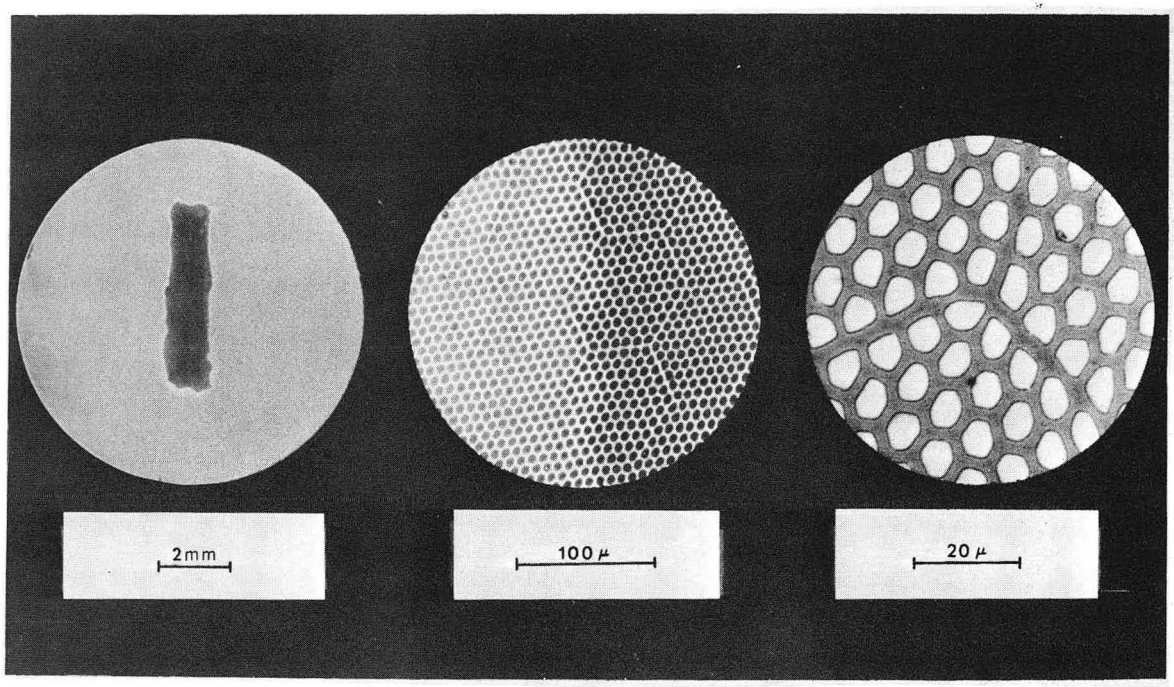


XBB 707-3371

Fig. 10

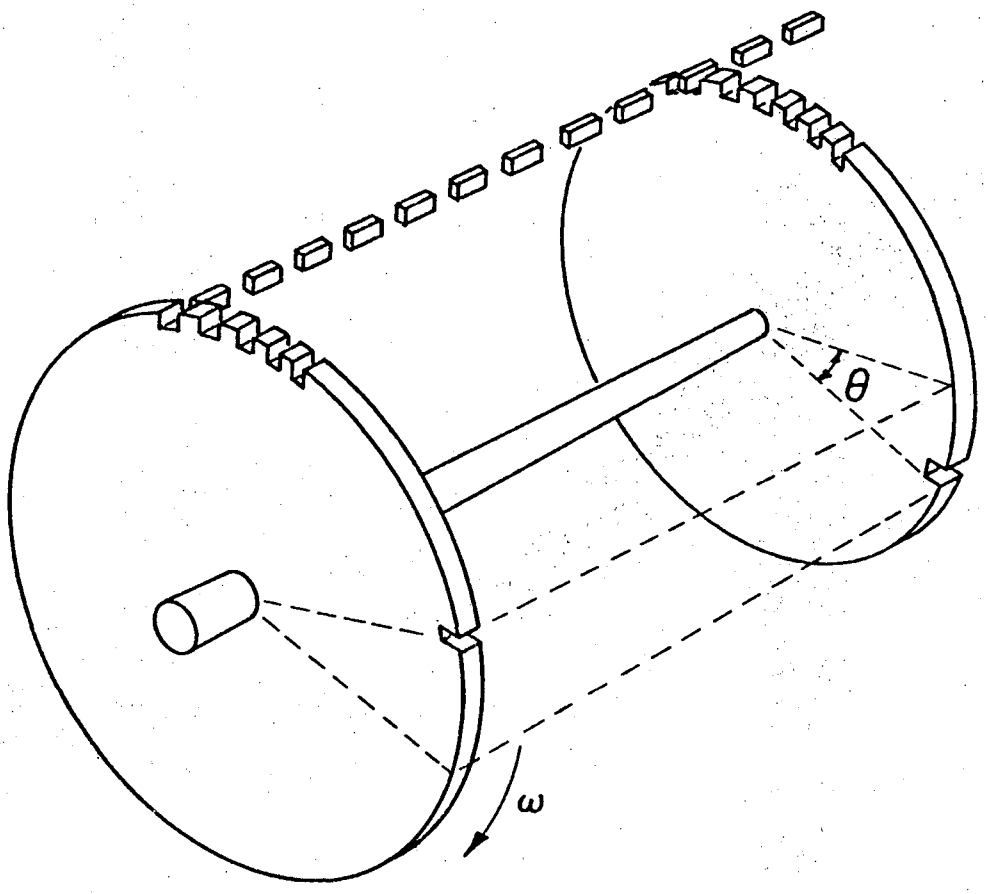


XBL708-3771

Fig. 11

Ion Gauge, Flux Sensitive Detector

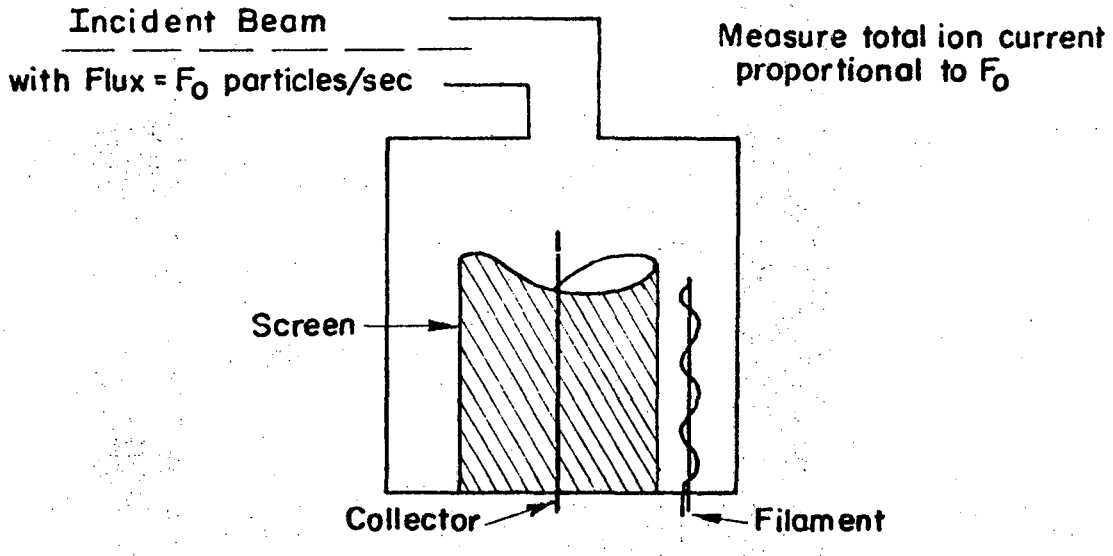


Mass Spectrometer, Density Sensitive Detector

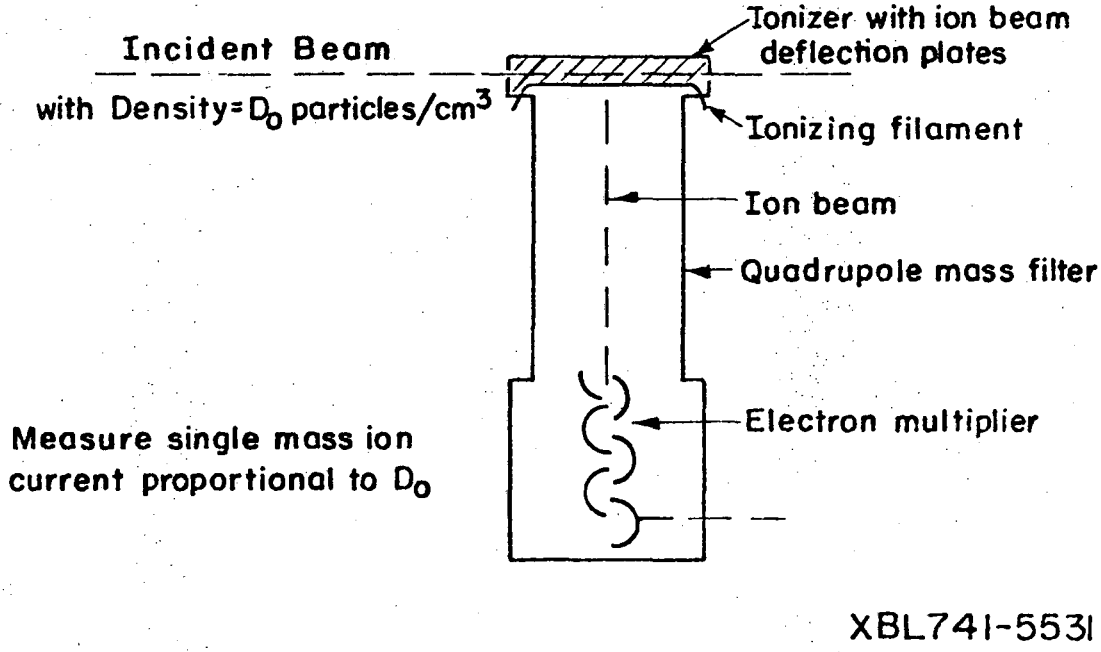


Fig. 12

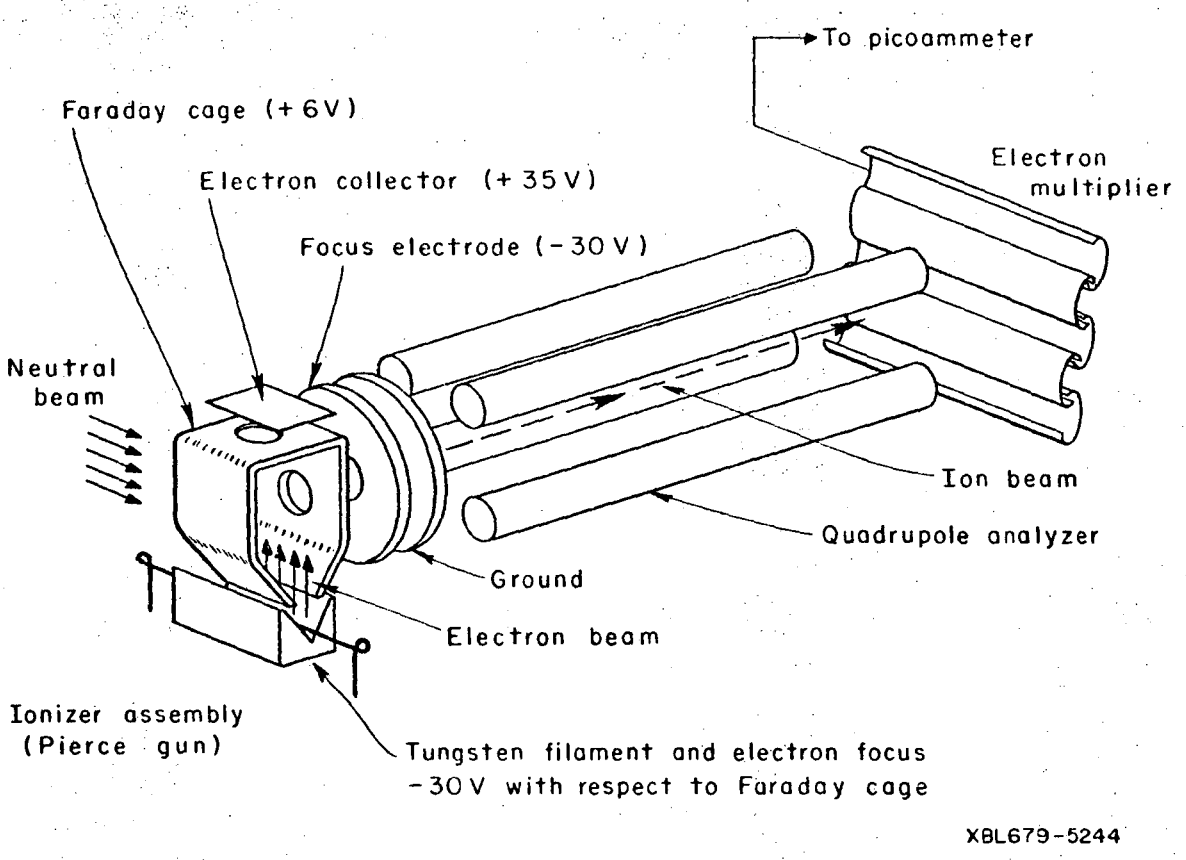
To picoammeter
Faraday cage (+6V)
Electron collector (+35V)
Focus electrode (-30V)
Electron multiplier
Neutral beam
Ion beam
Quadrupole analyzer
Ground
Electron beam
Ionizer assembly (Pierce gun)
Tungsten filament and electron focus -30V with respect to Faraday cage
XBL679-5244

Fig. 13

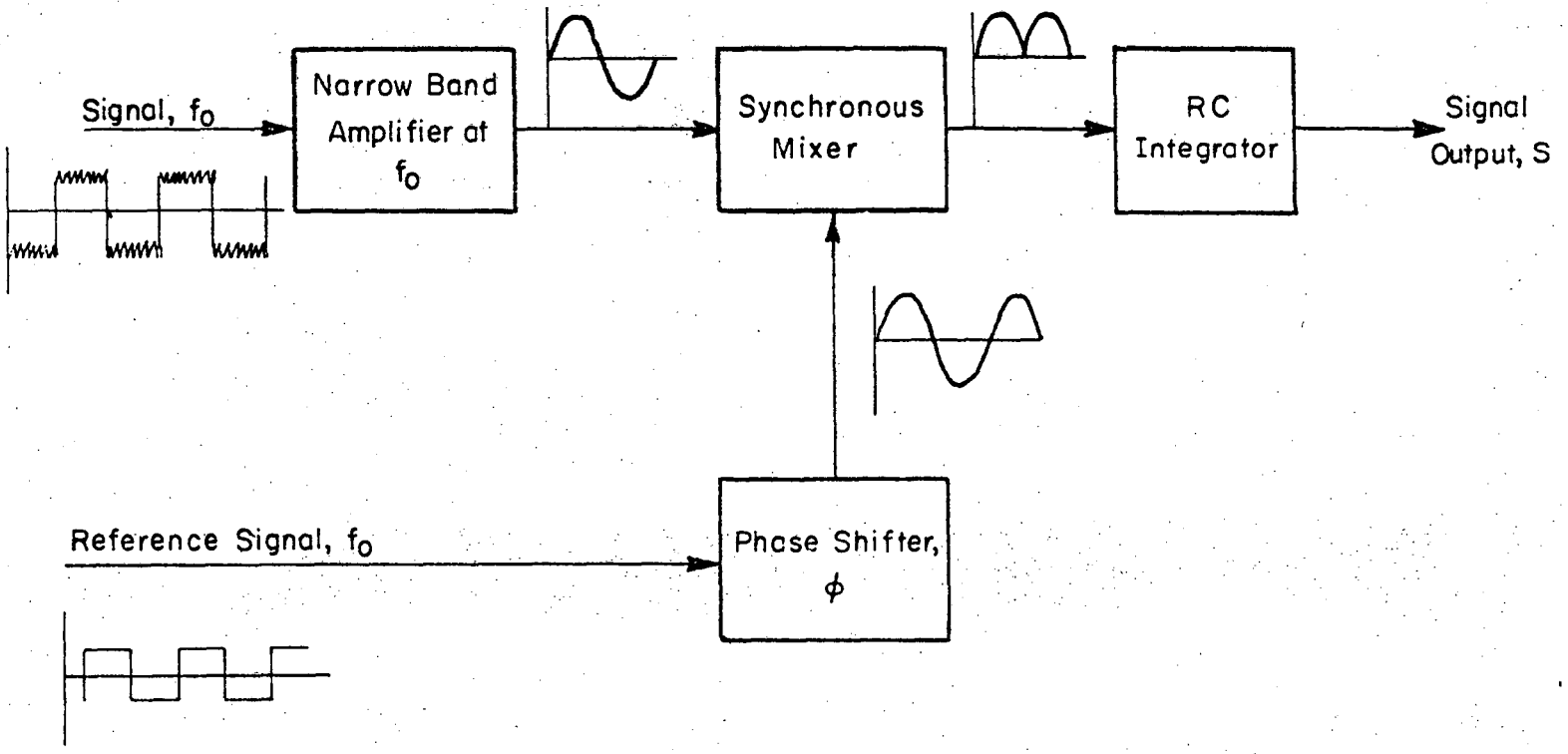


XBL 741-5532

Fig. 14

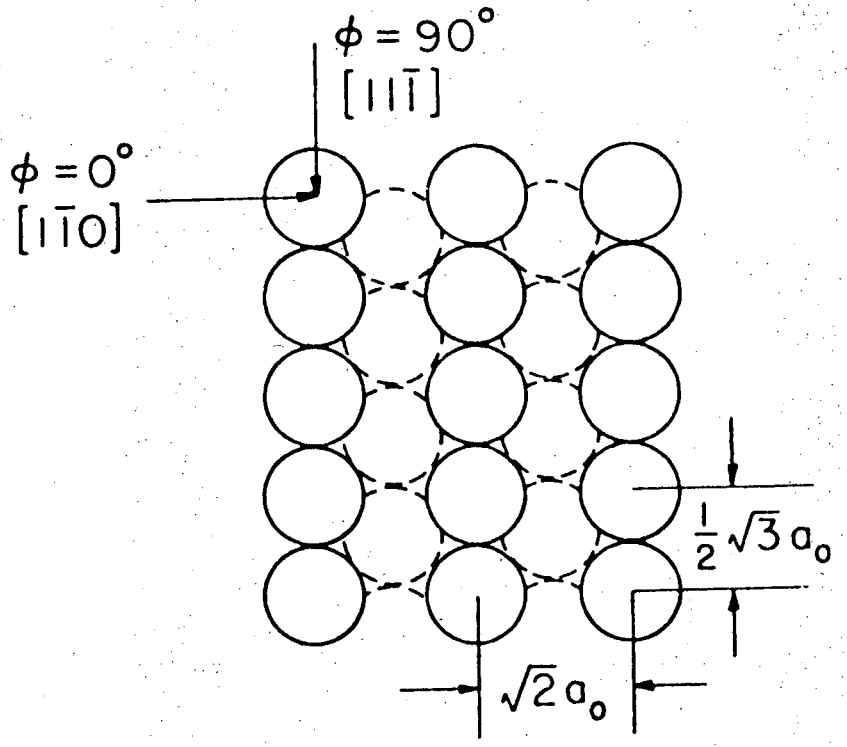


(a)
TOP VIEW
$a_o = 3.16$ Å

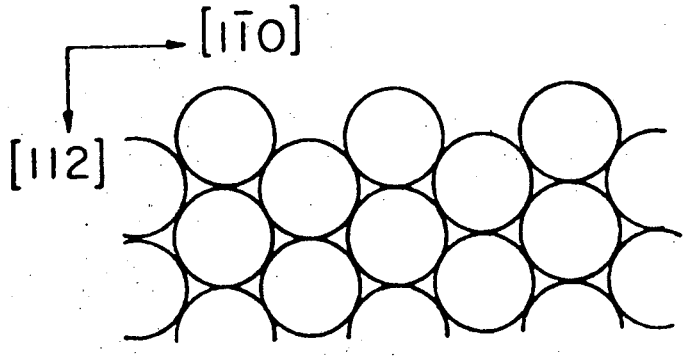


(b)
SIDE VIEW

XBL 738-1059

Fig. 15

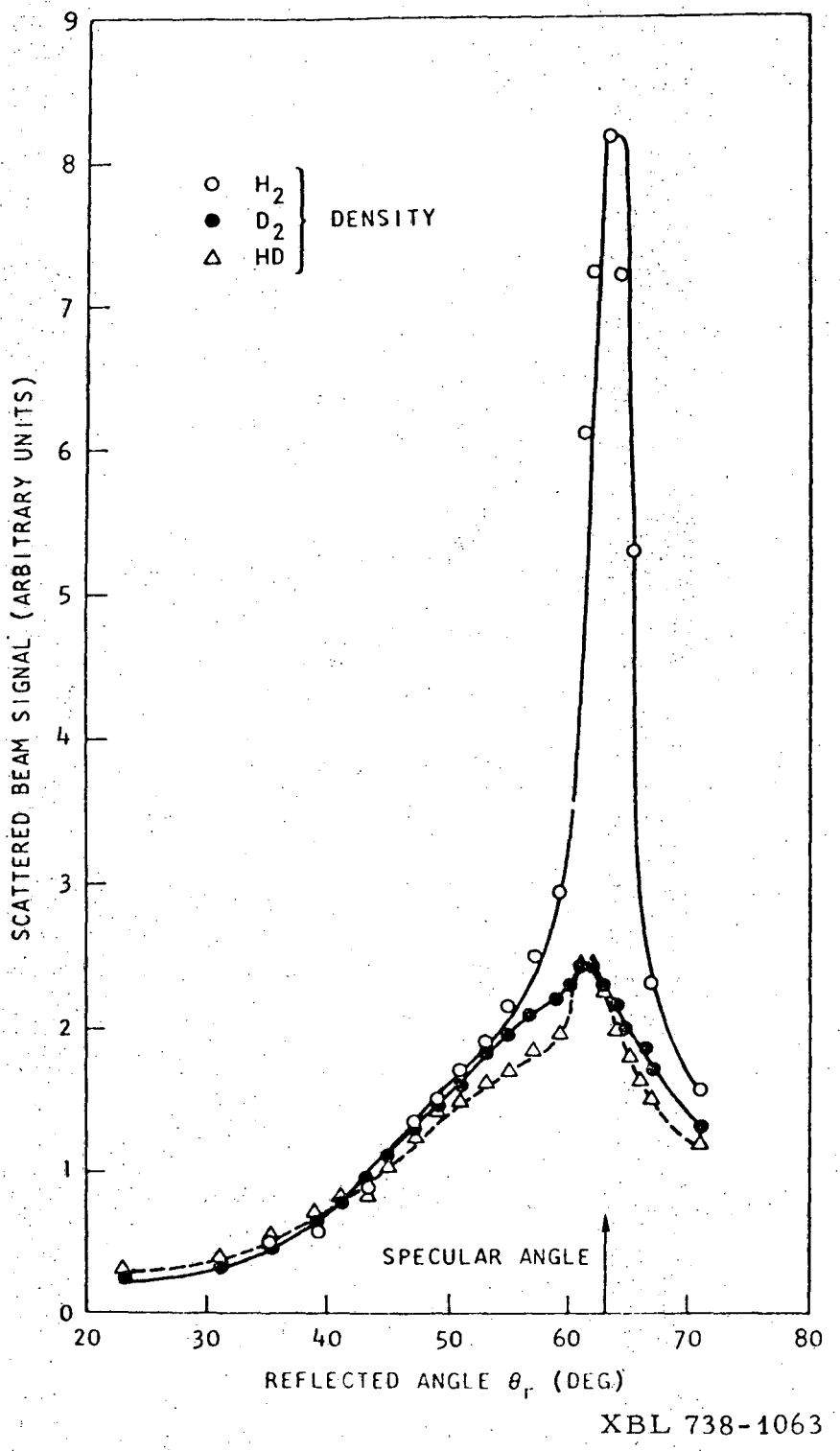
9
8
7
6
5
4
3
2
1
0
20
30
40
50
60
70
80
SCATTERED BEAM SIGNAL (ARBITRARY UNITS)
REFLECTED ANGLE $\theta_r$ (DEG.)
$H_2$
$D_2$
HD
DENSITY
SPECULAR ANGLE
XBL 738-1063

Fig. 16

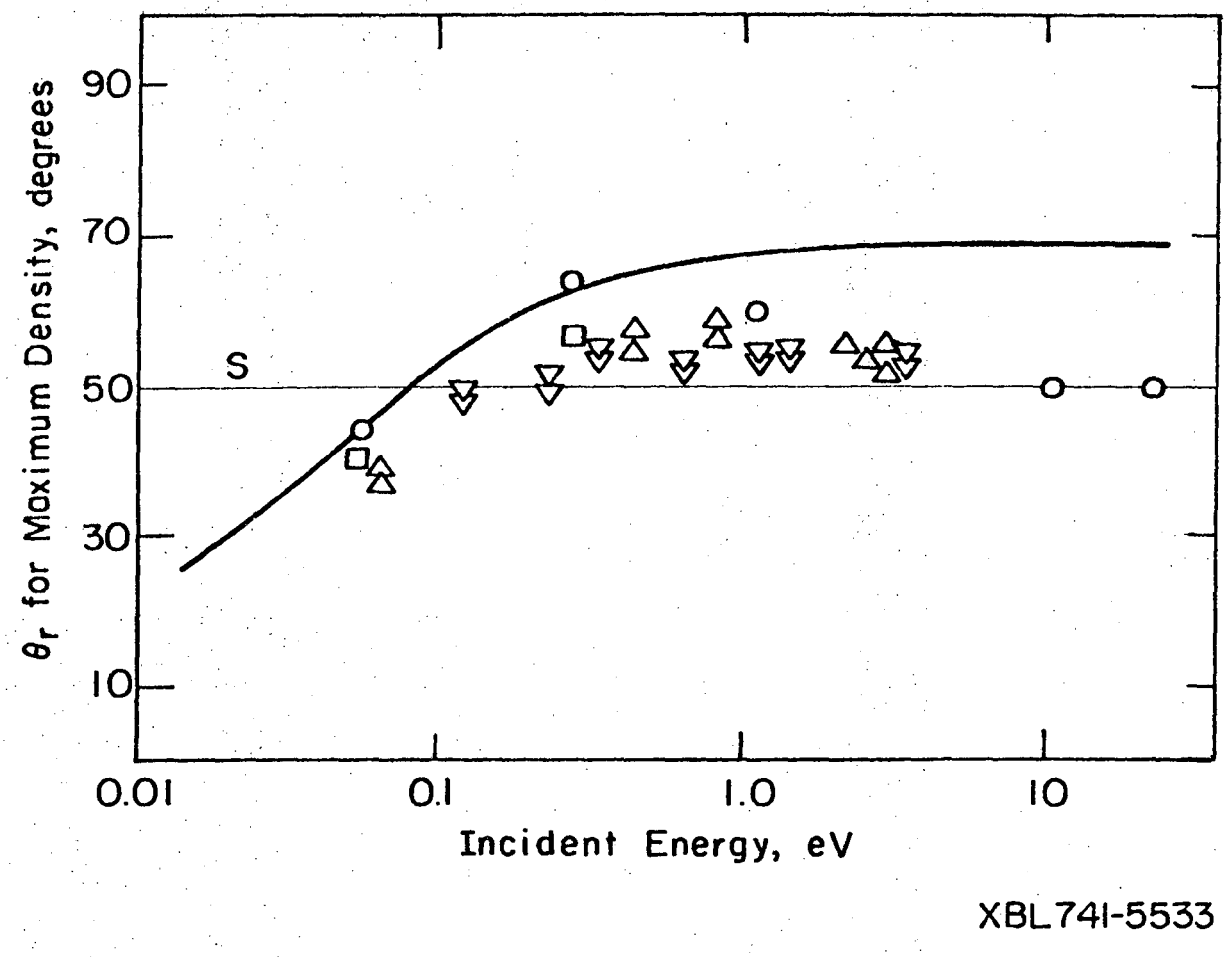
90
70
50
30
10
S
$\theta_r$ for Maximum Density, degrees
0.01
0.1
1.0
10
Incident Energy, eV
XBL741-5533

Fig. 17

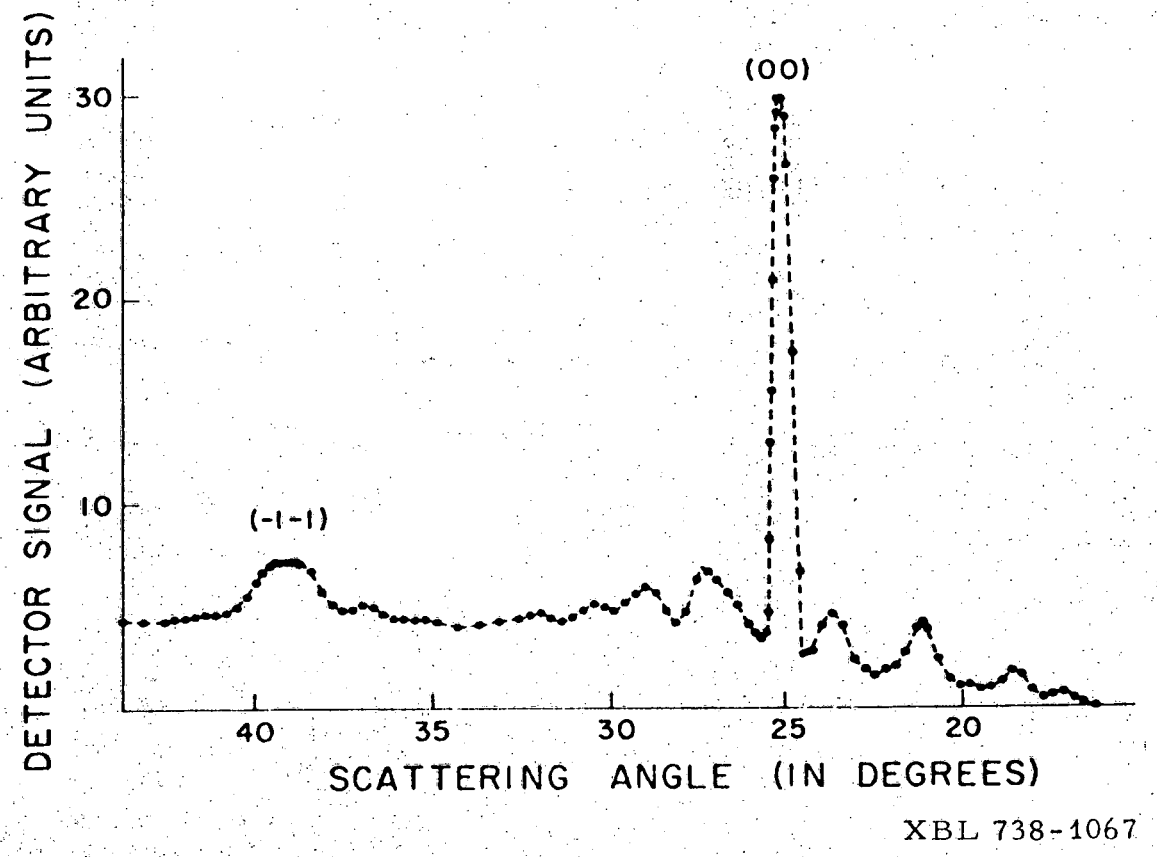
DETECTOR SIGNAL (ARBITRARY UNITS)
30
20
10
(00)
(-1-1)
40
35
30
25
20
SCATTERING ANGLE (IN DEGREES)
XBL 738-1067

Fig. 18

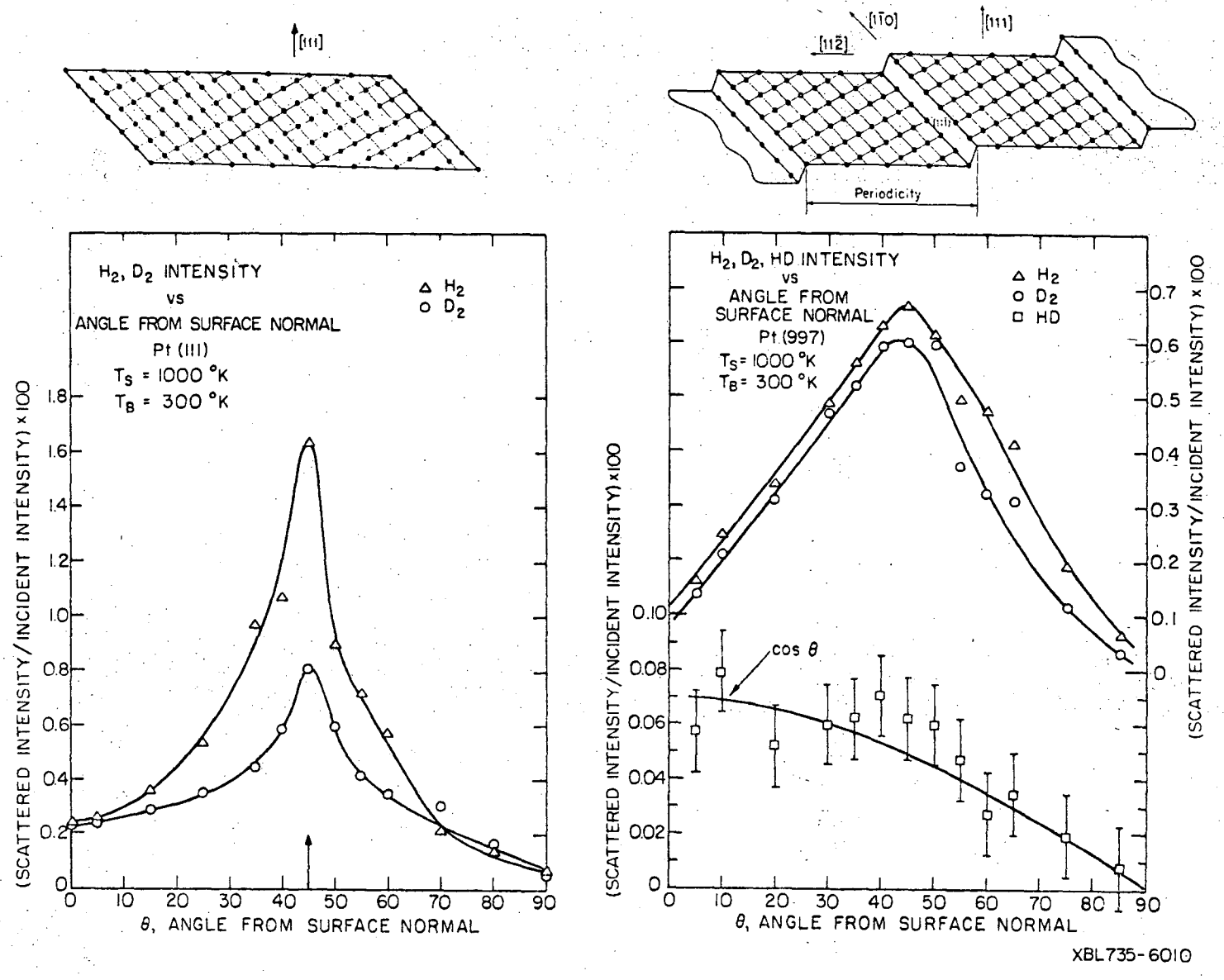
[111]
[1$\bar{1}$0]
[11$\bar{2}$]
[111]
Periodicity
$H_2$, $D_2$ INTENSITY
vs
ANGLE FROM SURFACE NORMAL
Pt (111)
$T_S$ = 1000 °K
$T_B$ = 300 °K
$H_2$
$D_2$
(SCATTERED INTENSITY/INCIDENT INTENSITY) x100
θ, ANGLE FROM SURFACE NORMAL
$H_2$, $D_2$, HD INTENSITY
vs
ANGLE FROM
SURFACE NORMAL
Pt (997)
$T_S$= 1000 °K
$T_B$= 300 °K
$H_2$
$D_2$
HD
cos θ
(SCATTERED INTENSITY/INCIDENT INTENSITY) x100
(SCATTERED INTENSITY/INCIDENT INTENSITY) x 100
θ, ANGLE FROM SURFACE NORMAL
XBL735-6010

Fig. 19

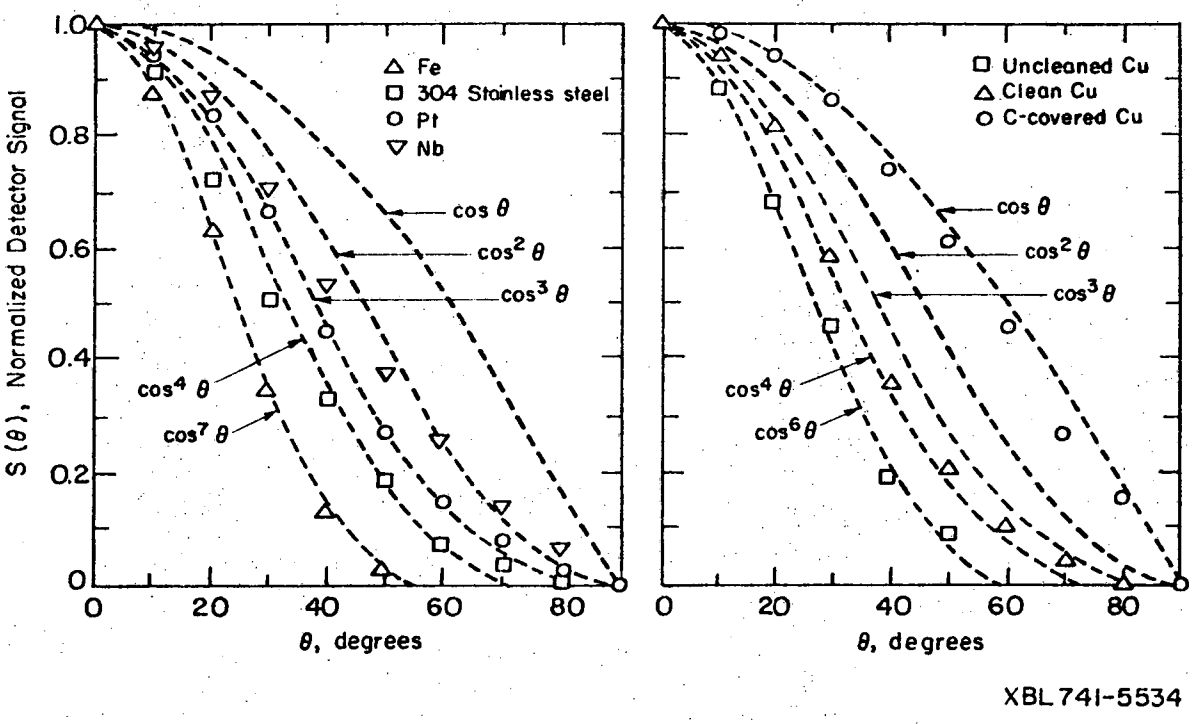
S (θ), Normalized Detector Signal
θ, degrees
Fe
304 Stainless steel
Pt
Nb
cos θ
cos² θ
cos³ θ
cos⁴ θ
cos⁷ θ
Uncleaned Cu
Clean Cu
C-covered Cu
cos⁶ θ
XBL 741-5534

Fig. 20

TECHNICAL INFORMATION DIVISION
LAWRENCE BERKELEY LABORATORY
UNIVERSITY OF CALIFORNIA
BERKELEY, CALIFORNIA 94720